Fatigue

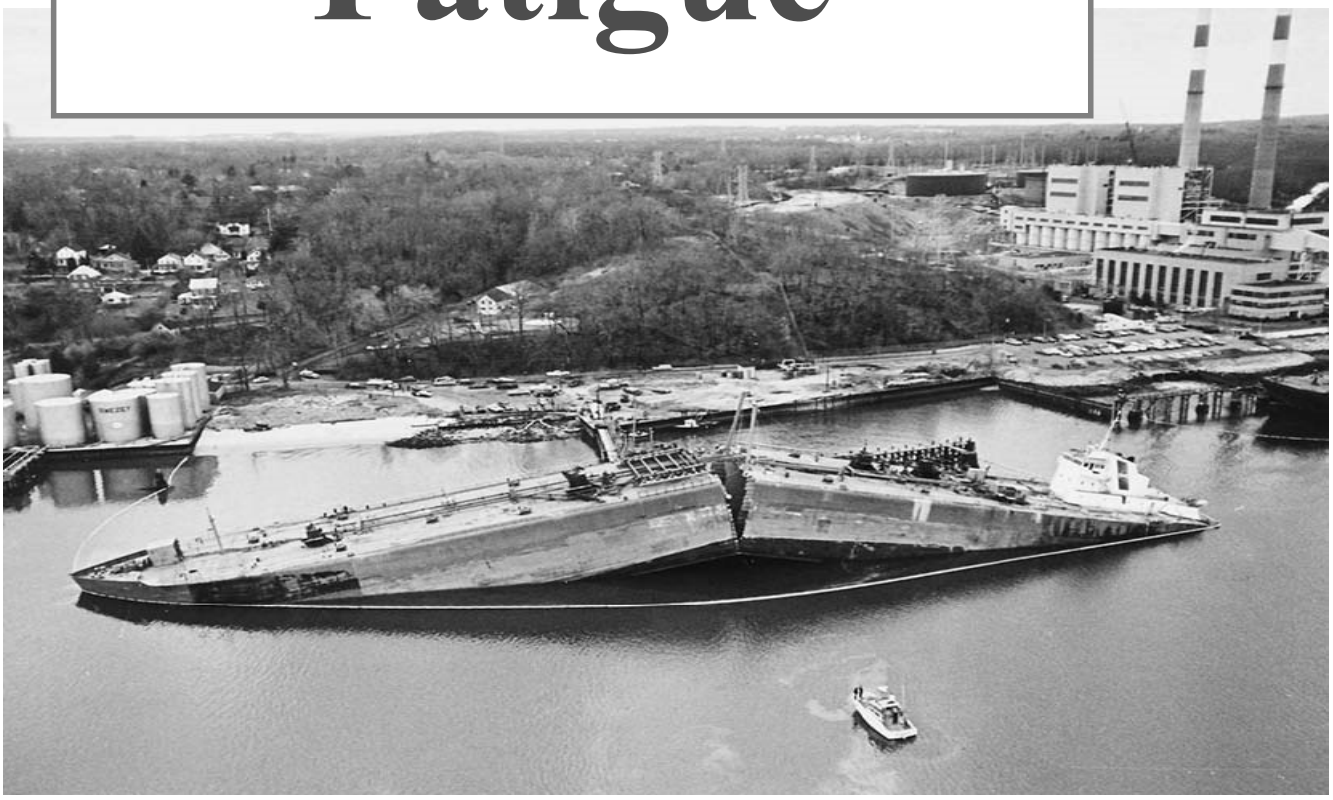

Cyclic Fatigue

Cyclic Fatigue of a Bridge

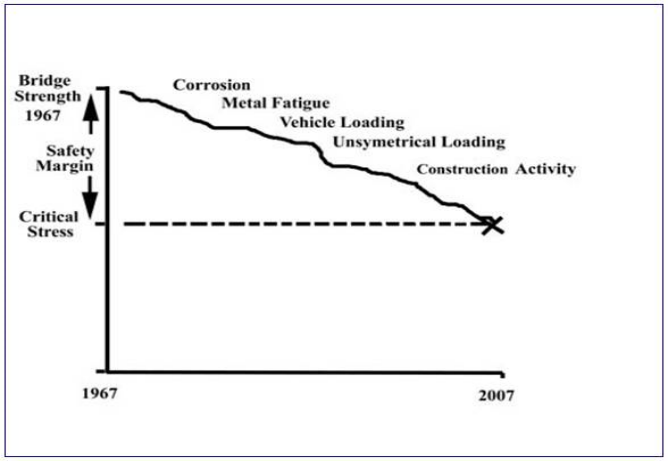

I35W bridge in Minneapolis on August 1, 2007

Fatigue cracks were observed.
Additionally also corrosion was acting
and one had asymmetric loads.

August Wöhler

On October 19, 1875 the locomotive *Amstetten* had an accident on the route between Salzburg and Linz because of a broken wheetset axle. The railroad administration demanded an investigation to figure out the causes of the disaster. August Wöhler, who at that time was preparing the new railway track from Hannover to Hamburg and who later worked for the Borsig family, took this accident as an occasion to submit shafts to a cyclic load and noticed, that their fatigue strength was considerably lower than their static strength, which was in fact the only quantity considered during this time. He was the first to make systematic studies of material fatigue.

1819 - 1914

Wöhler Curve

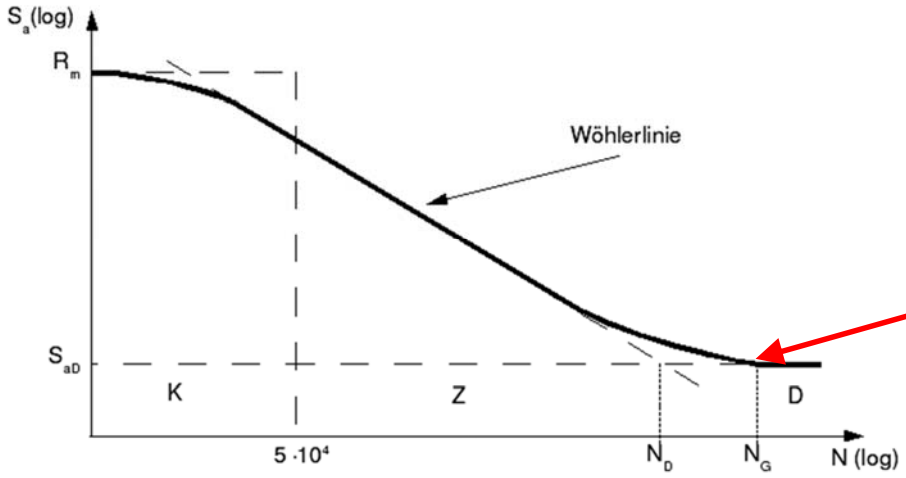

low cycle fatigue
«Kurzeitfestigkeit»

fatigue resistance
«Zeitfestigkeit»

fatigue strength
«Dauerfestigkeit»

L.F. Coffin (1954)
S.S. Manson (1953)

O.H. Basquin (1910)

Cyclic Fatigue of Metals

Crack initiation at a surface wrinkle («Scherlippe»)

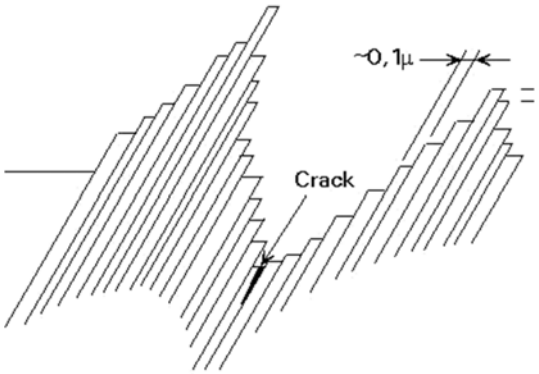

Step-like formation of a crack due to activation of gliding planes under symmetric changes between tension and compression

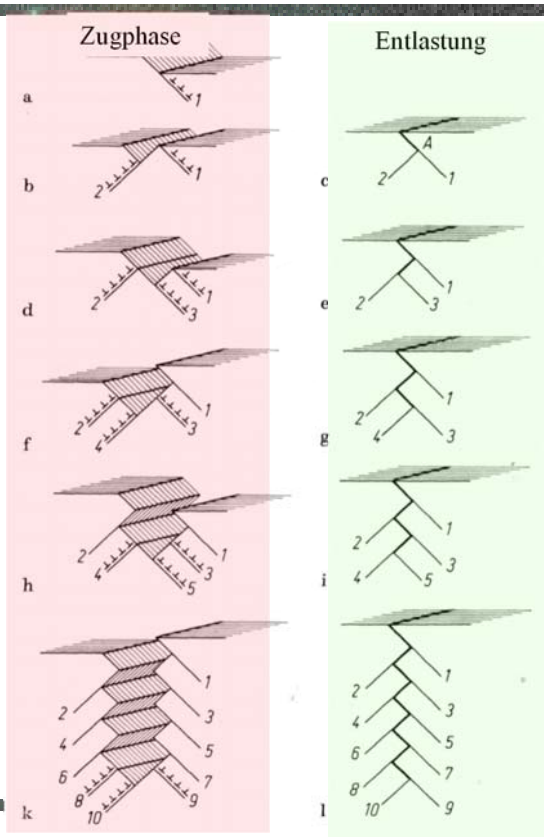

Cyclic Fatigue of Metals

- Microscopically fatigue consists in the accumulation of dislocations in shear bands.
- On the surface of the samples one can recognize this by the wrinkles („Scherlippen“) formed of extrusions and intrusions.
- In the case of LCF (low cyle fatigue) the yield stress is attained at each tension-compression cycle.

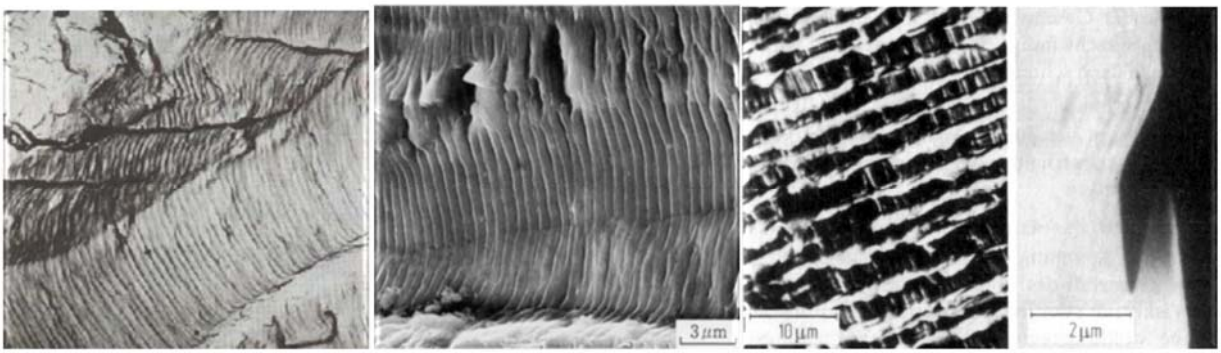

wrinkles on the crack surface

Growth Velocity of Fatigue Cracks: Paris(-Erdogan) Law

Relation between sub-critical crack growth velocity and the amplitude of the stress intensity factor (SIF):

$$\frac{da}{dN} = C\Delta K^m$$

$\Delta K = K_{max} - K_{min}$
C and m are material constants,
e.g. metals $2 < m < 7$; ceramics $20 < m < 100$

→ Prediction of the number of load changes that will yield to the failure of the sample.

Paris law is only vaild in regime II.

There exist many empirical laws for the crack growth in each regime.

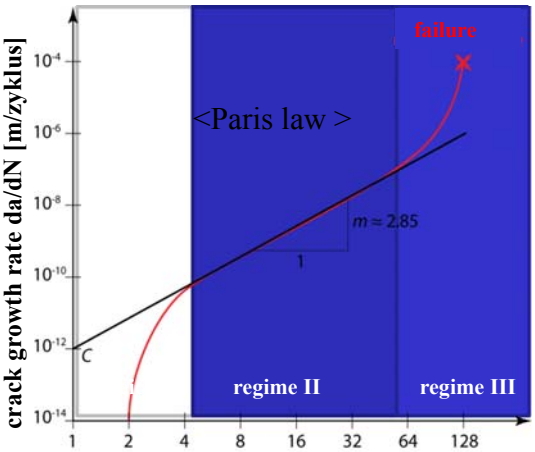

amplitude of the stress intensity factor [MPam$^{1/2}$]

P.C. Paris (1961)

(Walker, Forman, Collipriest, McEvily, Frost & Pook, Zheng, Wang, Miller & Gallgher, Dowling & Begley, Pugno)

Fatigue of Asphalt

Fatigue Test of Asphalt

4-Point Beam Bending Fatigue Test

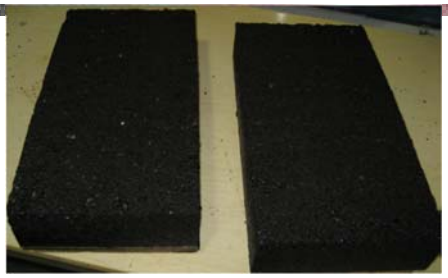

asphalt samples

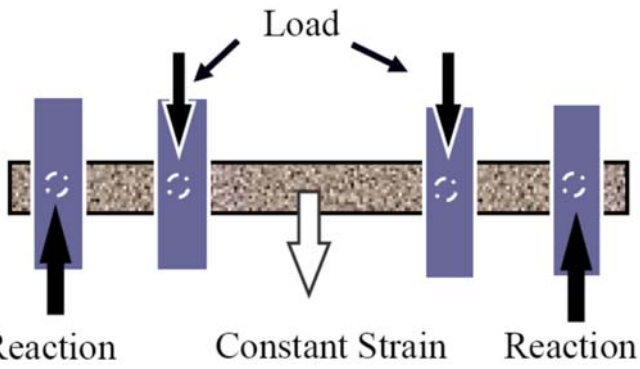

1 – 10 Hz

4-Point Beam Bending Fatigue Test

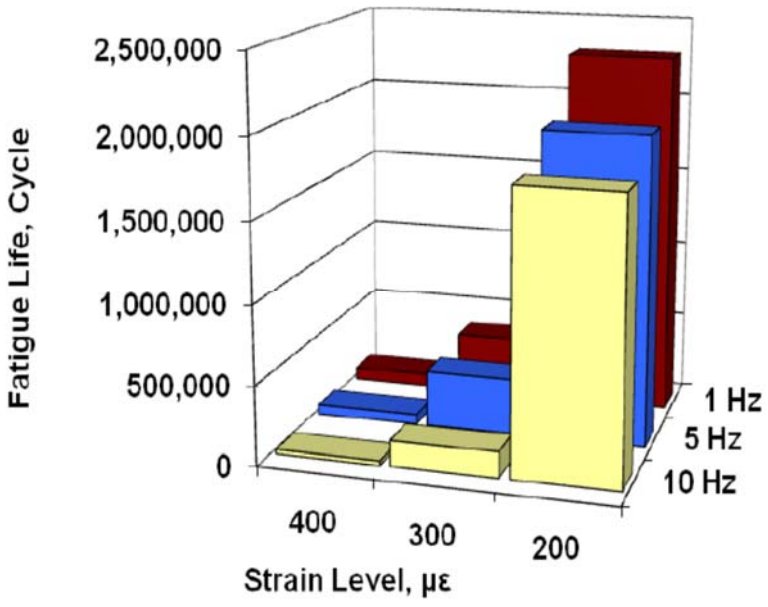

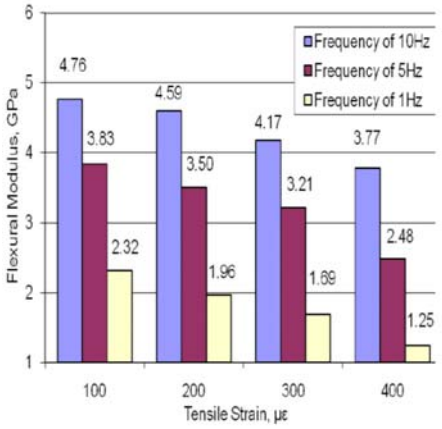

Testing Machine

strain controlled uni-axial
low-frequency tension

Fatigue Life Test for Asphalt

experimental setup

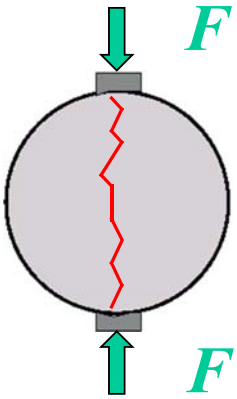

- cylindrical sample
- diametrical loading
- apply periodically

main observables

- evolution of deformation
- number of cycles to break

Brazil test

splitting tensile strength
«Spaltzugfestigkeit»

Experimental Setup

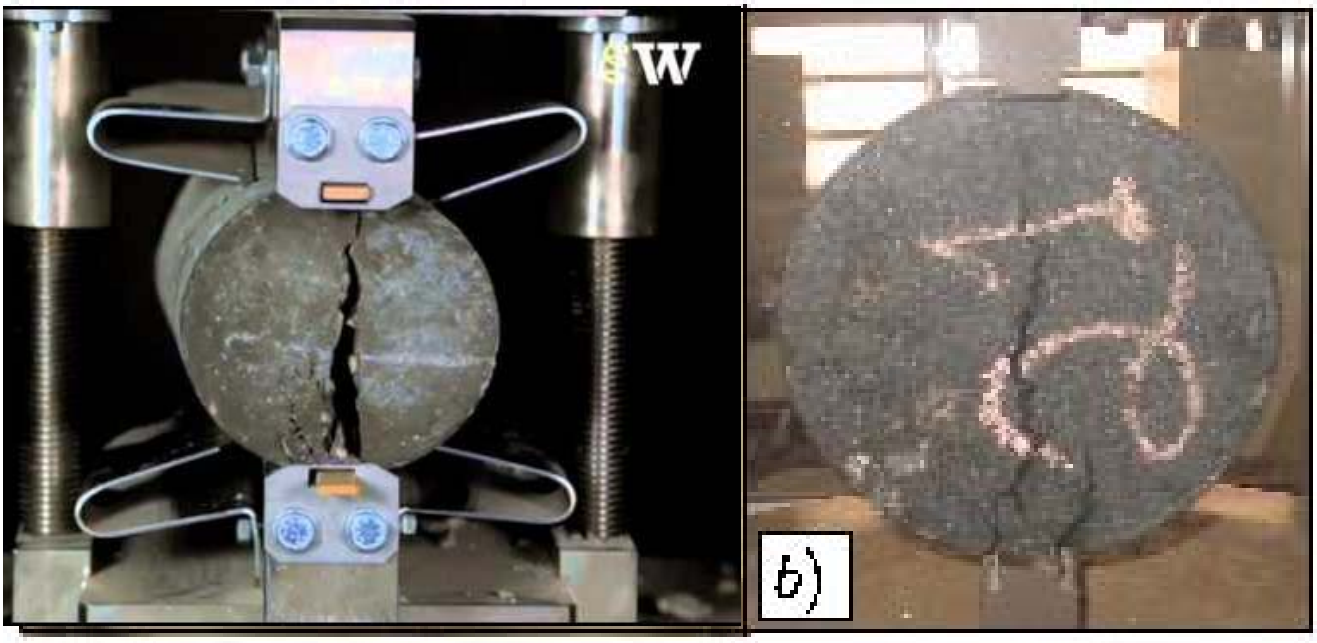

Laboratorio de pavimentos, Univ. Fed. do Ceará, Brasilien

Experimental Results

evolution of deformation

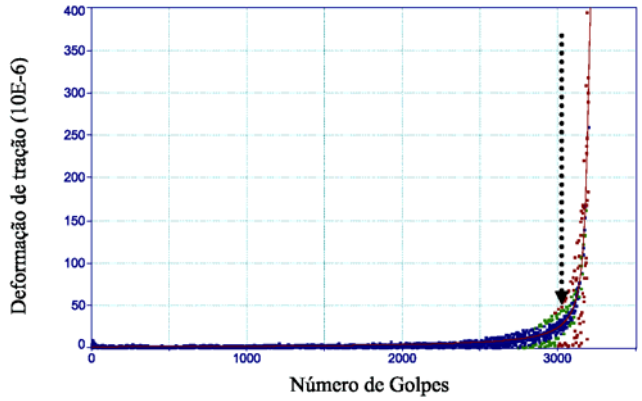

Basquin's law

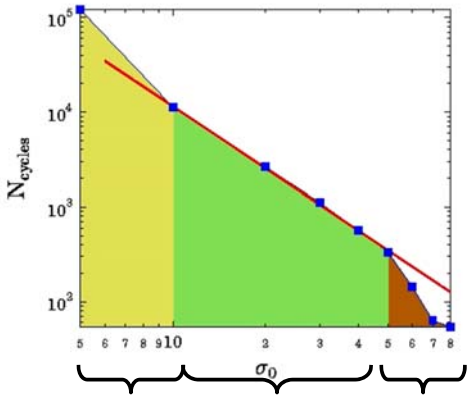

increase of life time | power law | immediate breaking

mechanisms

- immediate breaking
- damage accumulation
- healing
- viscoelasticity

low-frequency cycles: Coffin-Manson law

Fibre Bundle Model for Fatigue

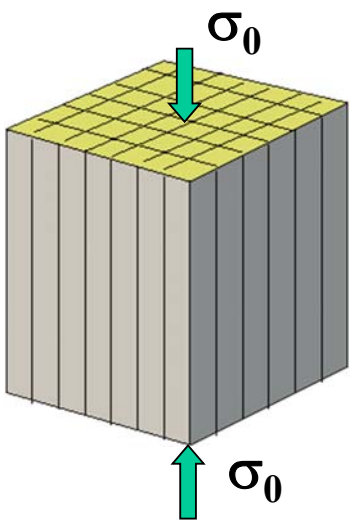

- parallel bundle of fibres
- constant external load σ_0
- time-independent response (no viscoelasticity)
- perfectly brittle behaviour of individual fibres
- interaction between fibres: equal load sharing

Brasil Test of Asphalt

arrangement of the fibres

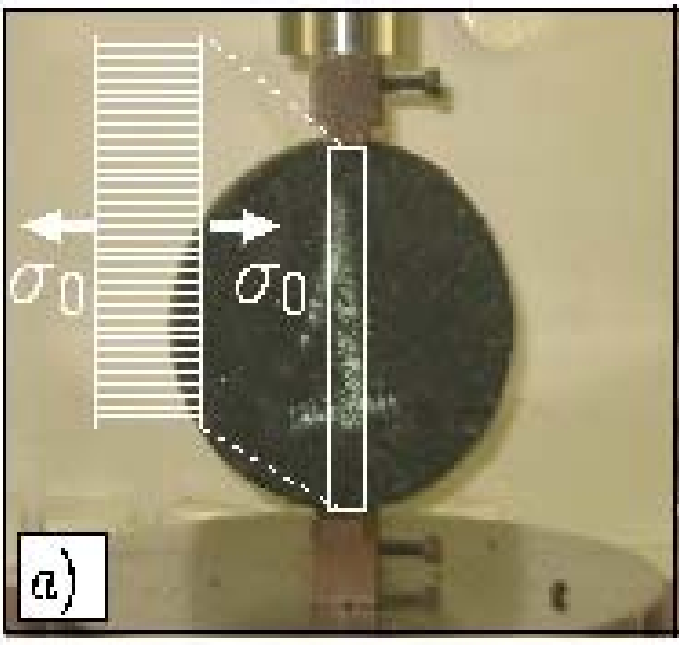

Microscopic Failure Mechanisms

failing due to two physical mechanisms

- brittle rupture, fails when $p_i > p_{th}^i$
- failure due to damage accumulation

$$\Delta c = \alpha_0 p^\gamma(t)\Delta t$$

nucleation rate of micro cracks

$$c(t) = \alpha_0 \int_0^t p^\gamma(t')dt'$$

dependence on history

$$c_i(t) > c_{th}^i$$

$$h(p_{th}, c_{th})$$

joint distribution

$$h(p_{th}, c_{th}) = g(p_{th}) f(c_{th})$$

- healing of damage

$$c(t) = \alpha_0 \int_0^t e^{-(t-t')/\tau} p^\gamma(t')dt'$$

τ limits the range of memory

Strain Stress Evolution

integral equation:

$$\sigma_0 = \left[1 - F\left(\alpha_0 \int_0^t e^{-(t-t')/\tau} p^\gamma(t')dt'\right)\right]\left[1 - G(p(t))\right] p(t)$$

damage accumulation and healing

static FBM

$\Rightarrow p(t)$

$p(t) = E\,\varepsilon(t)$

deformation

initial condition $\sigma_0 = [1 - G(p_0)]\, p_0 \Rightarrow p_0$

parameter of the model: γ, τ, α_0, σ_0/σ_c

Shortly before End of Life Time

$p(t)$

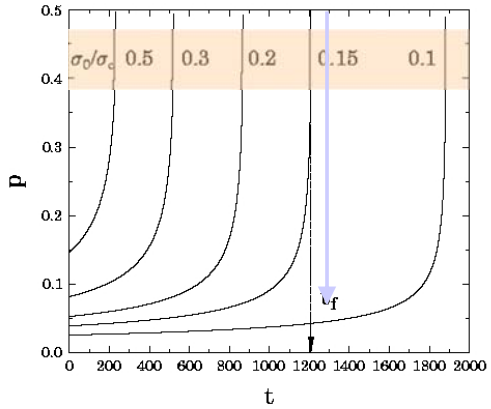

power law

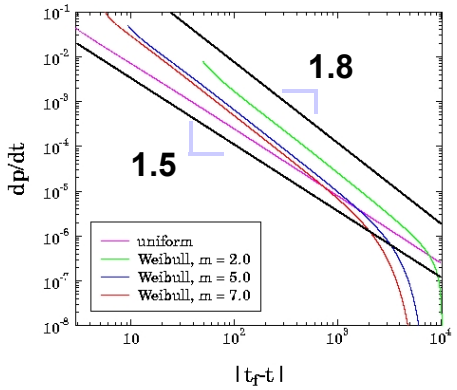

$$\frac{dp}{dt} \sim \left| t_f - t \right|^{-\beta}$$

disorder

- **finite** $\beta = 1.50 \pm 0.04$
- **infinite** $\beta = 1.80 \pm 0.06$

} **two different cases**

Life Time (Number of Cycles till Failure)

t_f **as function of** σ_0/σ_c

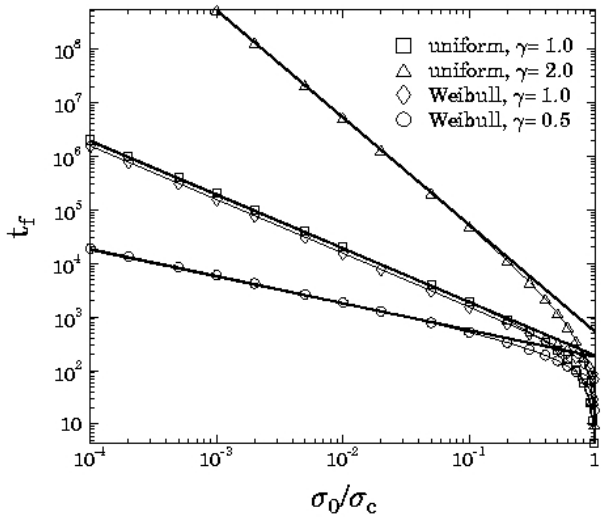

power law

$$t_f \sim \left(\frac{\sigma_0}{\sigma_c} \right)^{-\alpha}$$

with $\alpha = \gamma$

independent on the type of disorder

- **different distributions of disorder**
- **different exponents** γ

Effect of Healing

stress-strain evolution

$$\sigma_0 = \left[1 - F\left(\alpha_0 \int_0^t e^{-(t-t')/\tau} p^{\gamma}(t')dt'\right)\right]\left[1 - G(p(t))\right] p(t)$$

fixed σ_0/σ_c variable τ

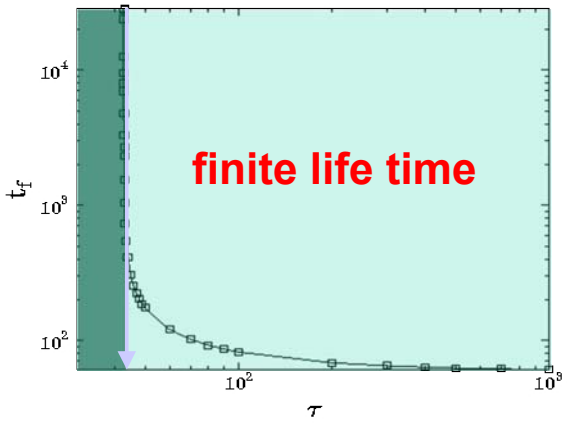

- τ limits the range of memory.
- competition between damage and healing
- τ_c separates two phases.

$\tau < \tau_c$ infinite life time

$\tau > \tau_c$ finite life time

Constant Maximal Load

phase diagram

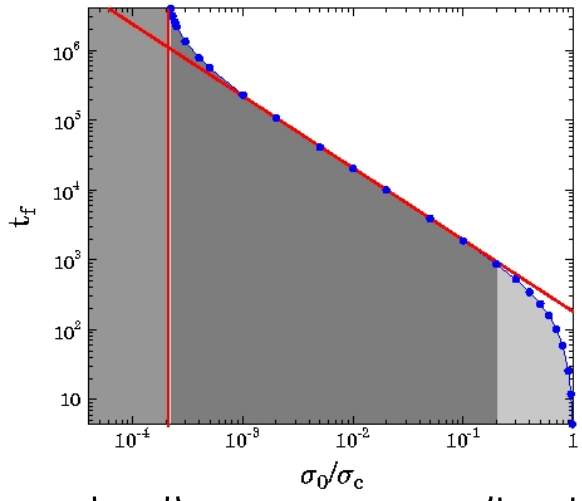

no failure power law rapid failure

different γ

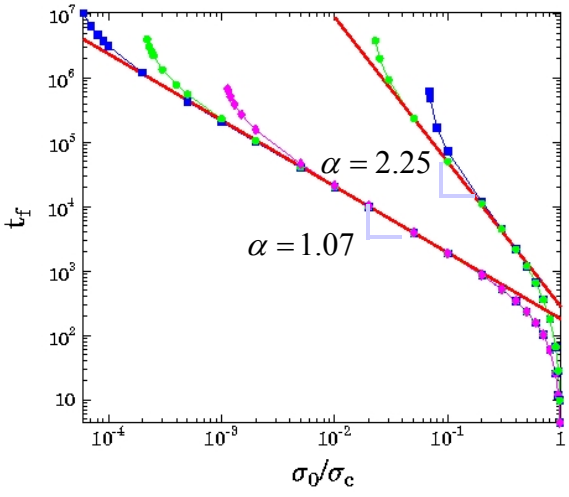

Life Time and Relaxation Time

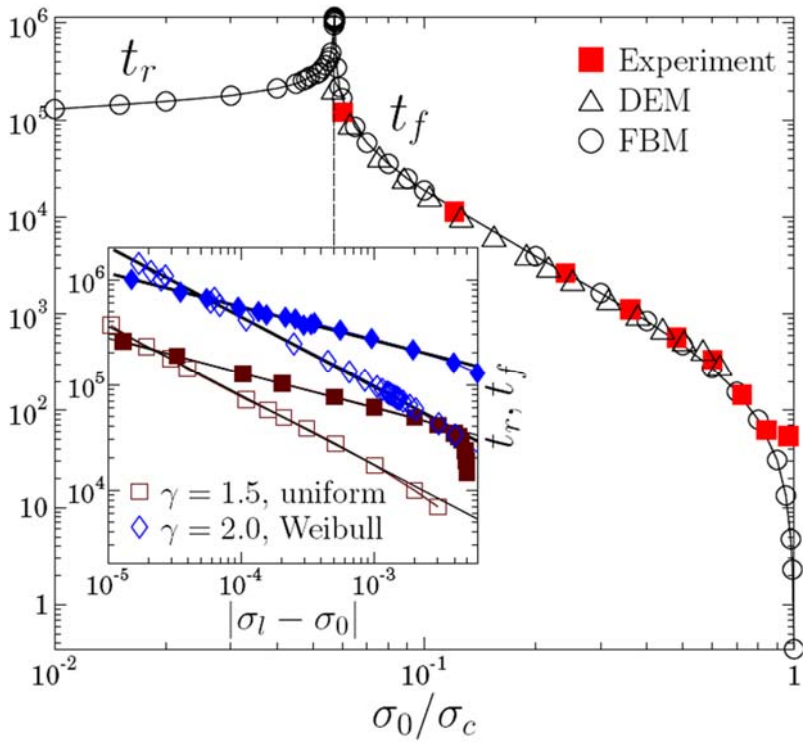

σ_l is load at threshold.

Below σ_l the stress relaxes to a finite value with a relaxation time t_r .

$$t_r \propto (\sigma_l - \sigma_0)^{-1/3}$$

$$t_f \propto (\sigma_0 - \sigma_l)^{-2/3}$$

DEM and Lattice Models

→ Discretization of Space

Beam Model

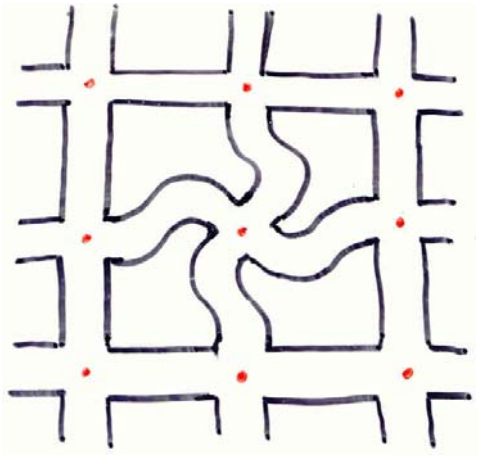

discretized (Cosserat) description of elasticity

on each site i: $x_i \quad y_i \quad \Theta_i$

$$z = \Theta l$$

cellular solid

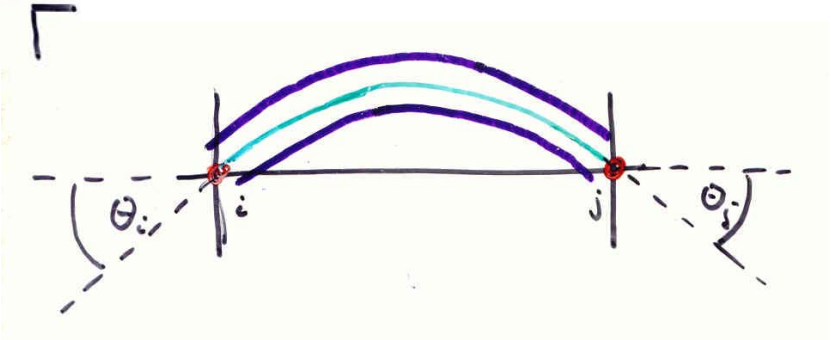

Breaking a Beam

Consider external shear

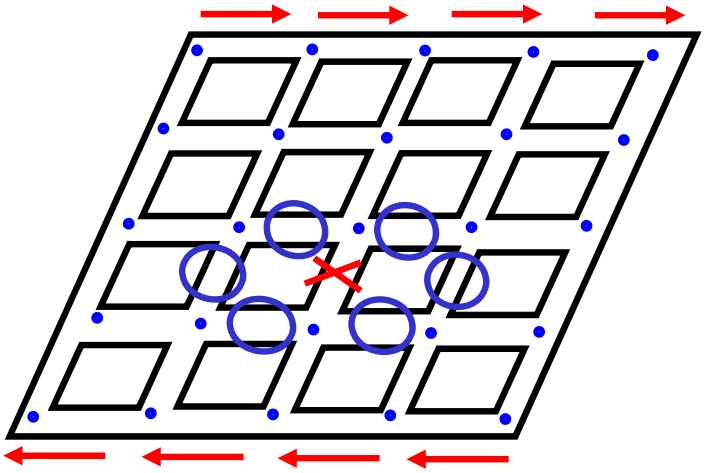

Can break by traction only or by bending

$$p = \left(F^2 + q \ \max\left(\left| M_i \right|, \left| M_j \right| \right) \right)$$

Discretization of the Sample

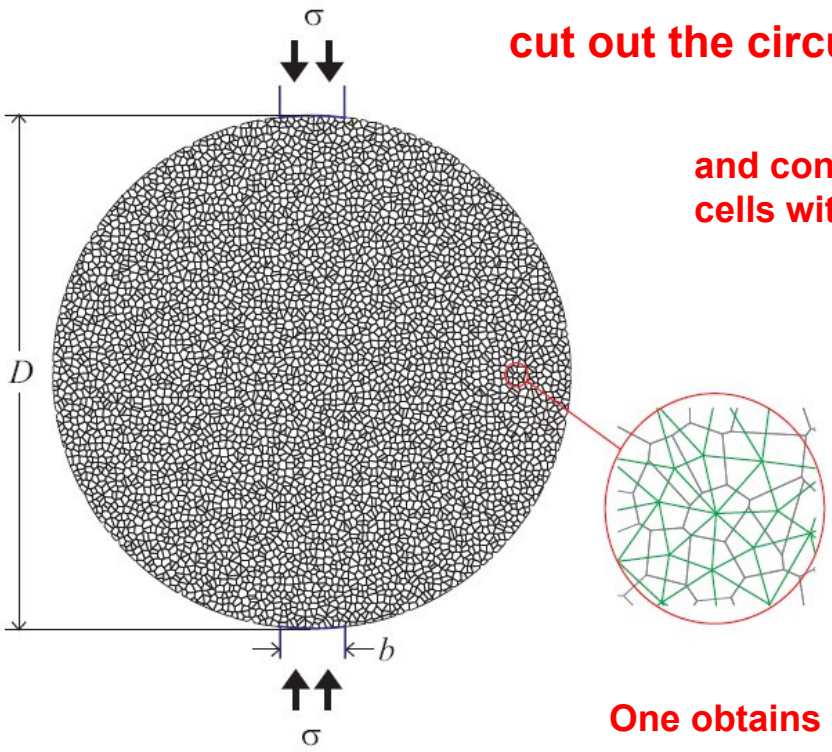

cut out the circular shape

and connect neighboring cells with beams.

One obtains a triangulation.

Breaking Criterion

previously:

$$p(t) = \left(\frac{F}{t_F} \right)^2 + \frac{\max\left(M_i, M_j\right)}{t_M}$$

damage accumulation **healing**

now replace p by q :

$$q(t) = p(t) + \alpha_0 \int_0^t e^{-\frac{t-t'}{\tau}} p(t')dt'$$

$$p(t) \geq 1 \quad \rightarrow \quad q(t) \geq 1$$

Parameters used in Simulation

Parameter		Value
Number of elements		5070
Density	ρ	$5\ g/cm^3$
Bulk Young modulus	Y	$1 \times 10^{10}\ dyn/cm^2$
Beam Young modulus	E	$5 \times 10^{10}\ dyn/cm^2$
Time step	δt	$1 \times 10^{-6}\ s$
Diameter of the disk	D	$20\ cm$
Typical size of a single element		$0.5\ cm$
Width of the load platen	b	$2.5\ cm$
Memory factor	α_0	$10 - 500$
Range of memory	τ	$500 - \infty$

Simulation of Brazil Test

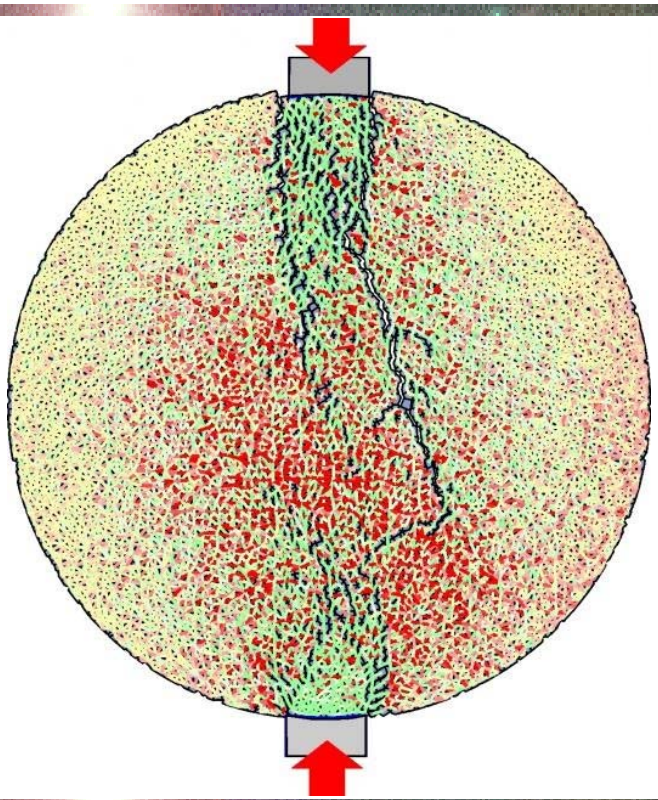

Simulation of Brazil Test

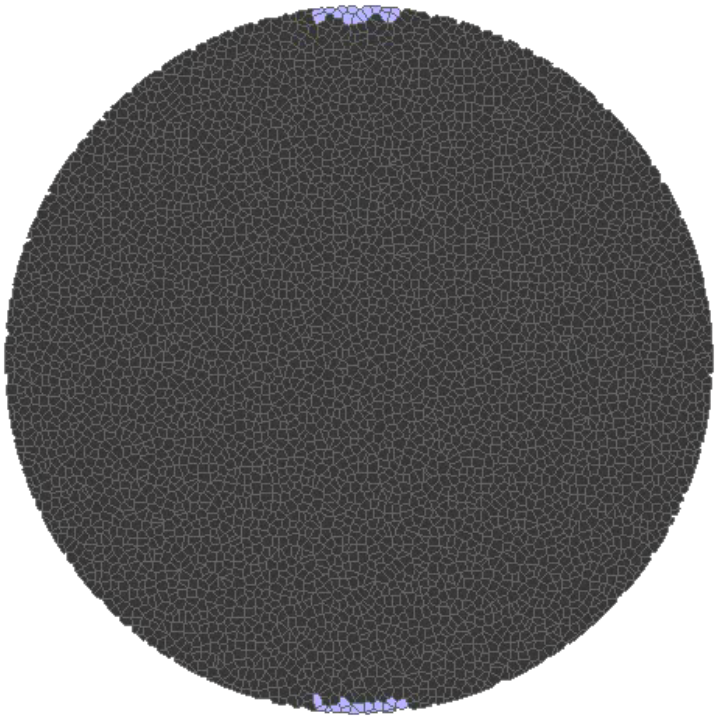

Simulation with more Disorder

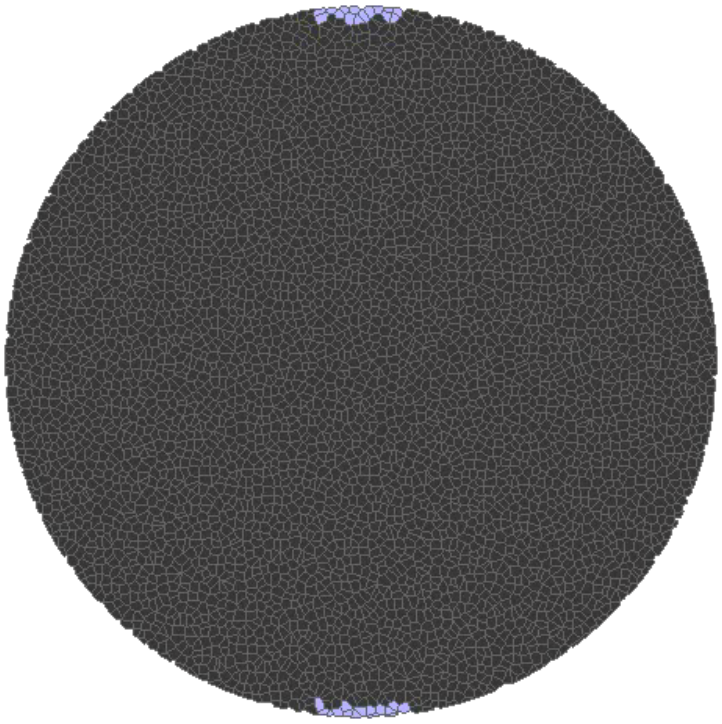

Time Evolution of Damage

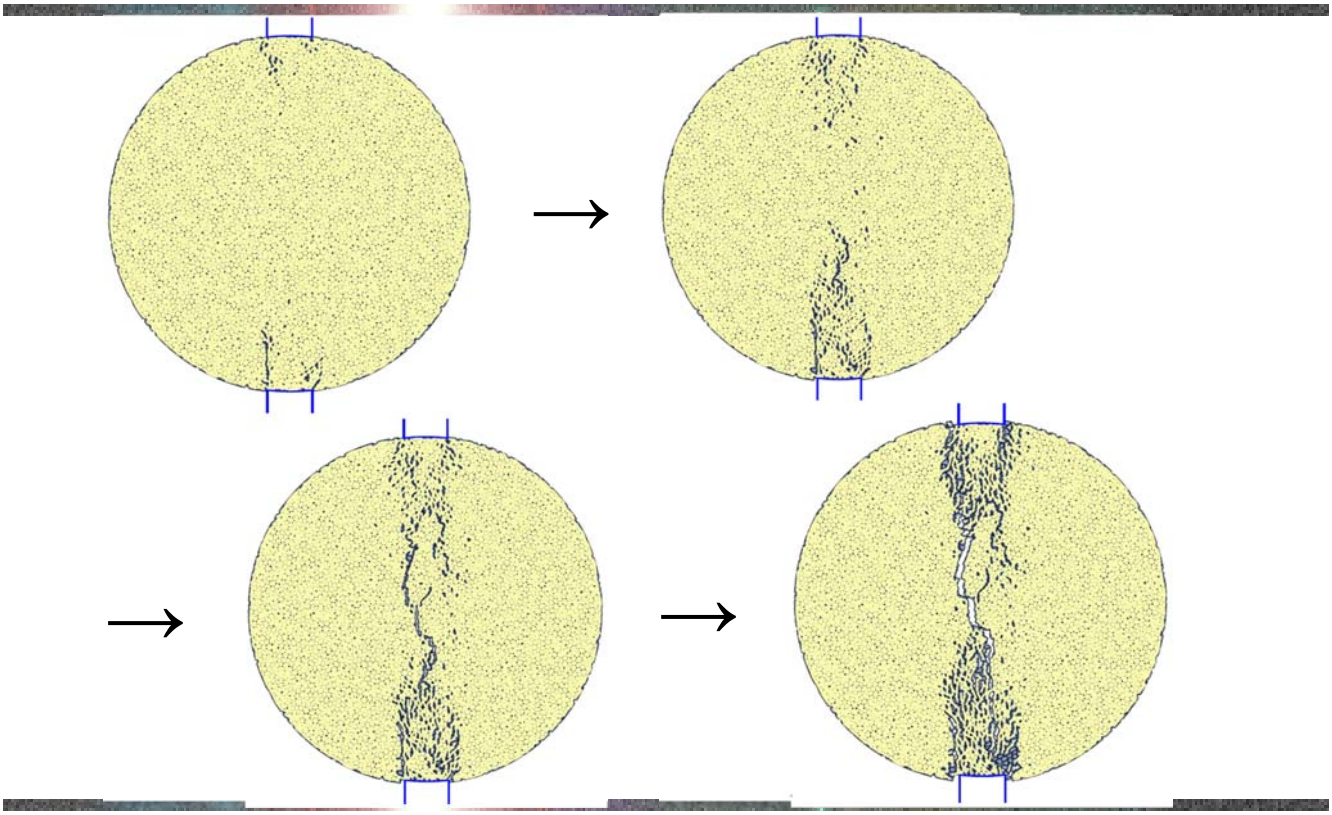

Dependence on Memory

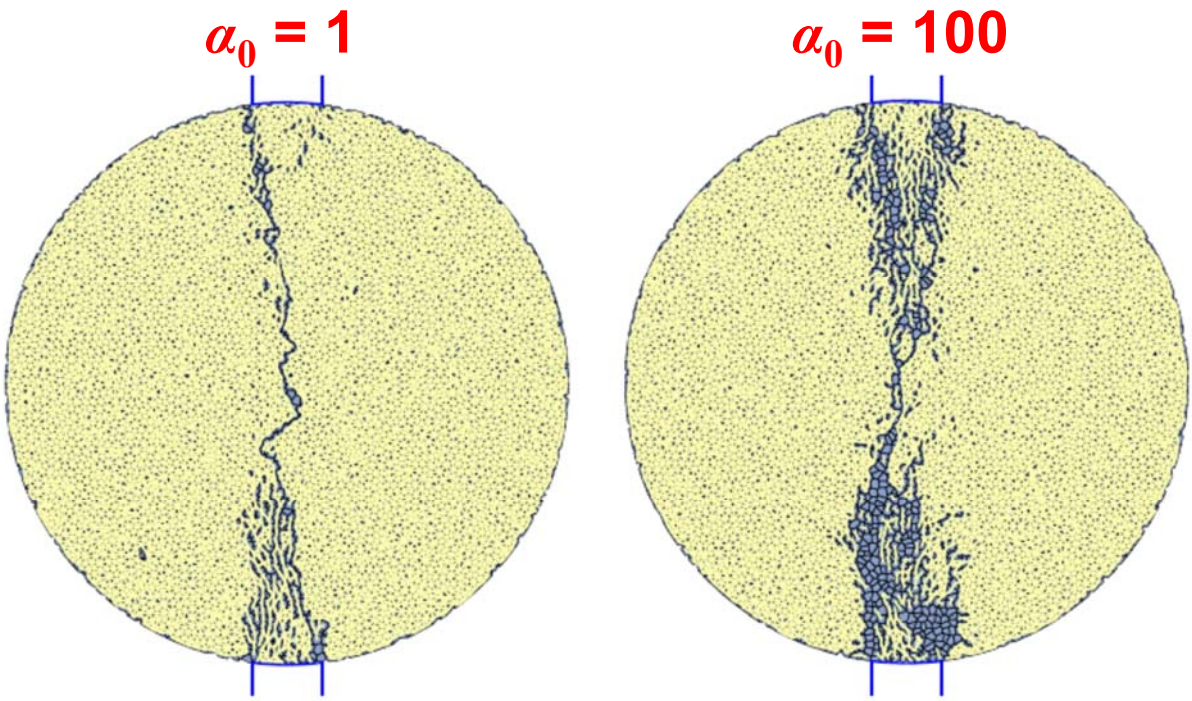

Deformation in Time

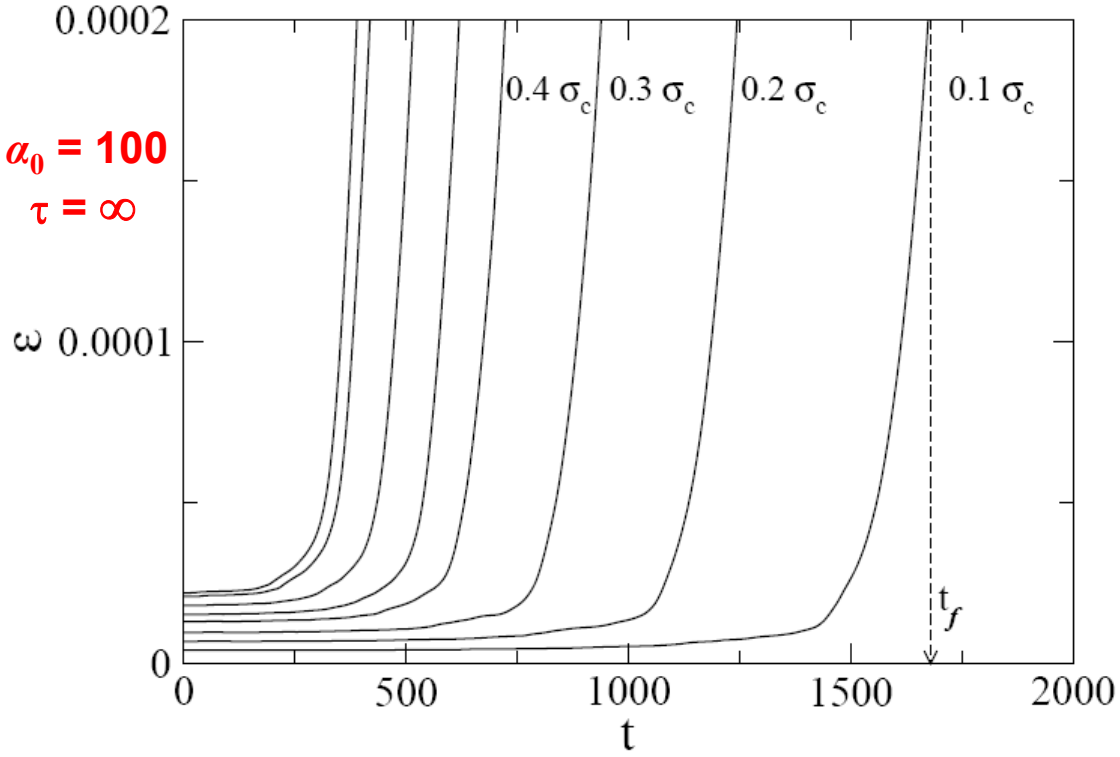

Comparison to Experiment

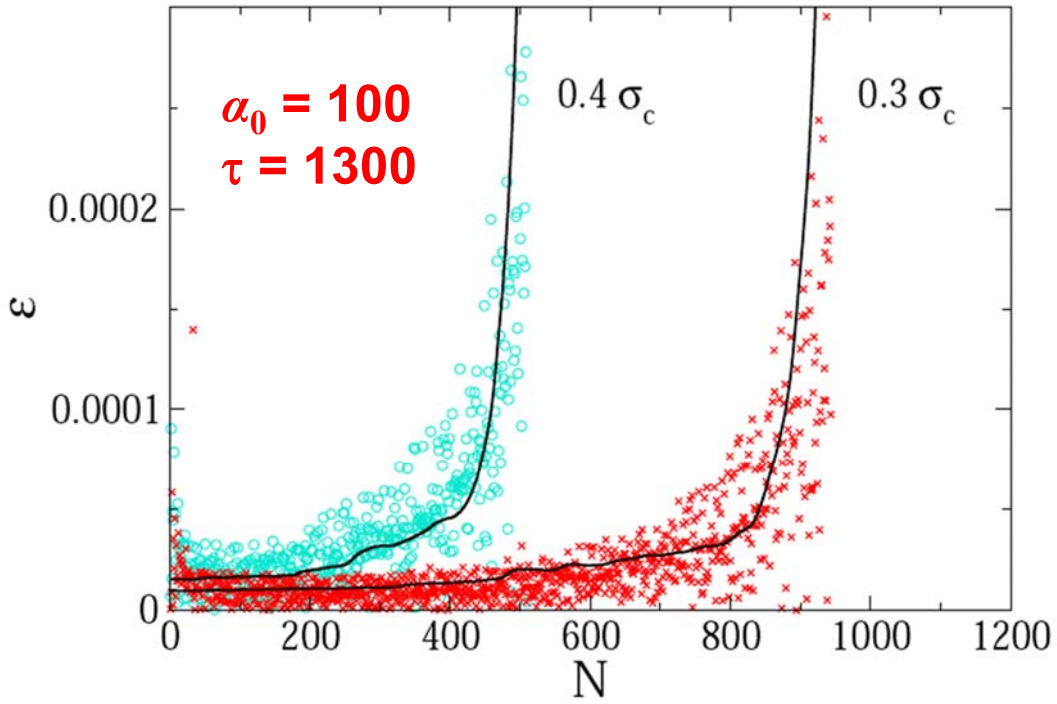

Dependence on healing time τ

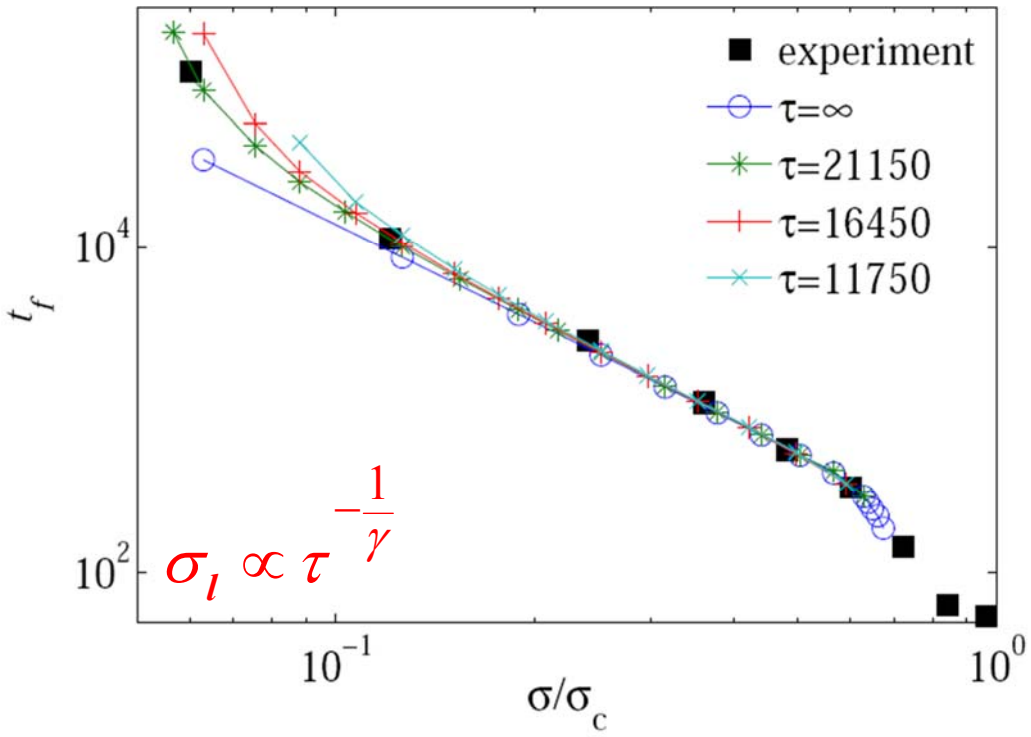

Life Time and Relaxation Time

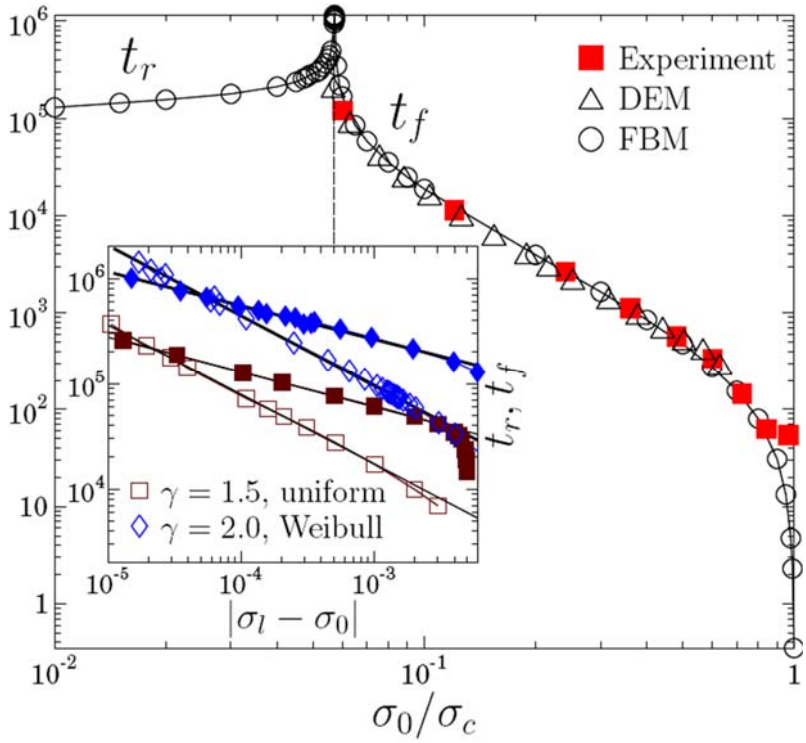

σ_l is load at threshold.

Below σ_l the stress relaxes to a finite value with a relaxation time t_r .

$$t_r \propto (\sigma_l - \sigma_0)^{-1/3}$$

$$t_f \propto (\sigma_0 - \sigma_l)^{-2/3}$$

Corrosion

Origin of Corrosion

- galvanic
- hydrogen embrittlement
- chloride ions and O_2 in solution
- bacteria

Stress Corrosion Cracking

metal

glas

concrete

Stress Corrosion Cracking

alloy	normal SIF	environment	reduced SIF
stainless steel	60 MN/m$^{3/2}$	3% NaCl	12 MN/m$^{3/2}$
brass	200 MN/m$^{3/2}$	ammonia	1 MN/m$^{3/2}$
Al(3Mg,7Zn)	25 MN/m$^{3/2}$	water (Cl^-)	5 MN/m$^{3/2}$
Cr Ni steel	200 MN/m$^{3/2}$	42% $MnCl_2$	10 MN/m$^{3/2}$

Stress Corrosion Cracking


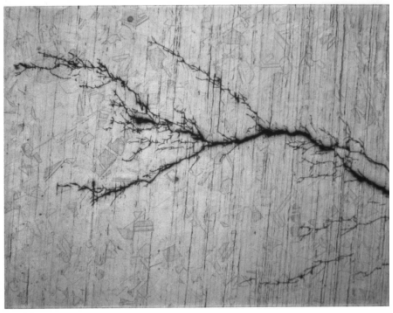


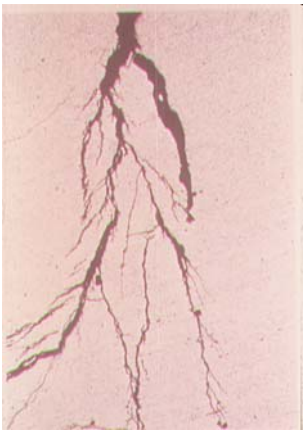

Stress Corrosion Cracking

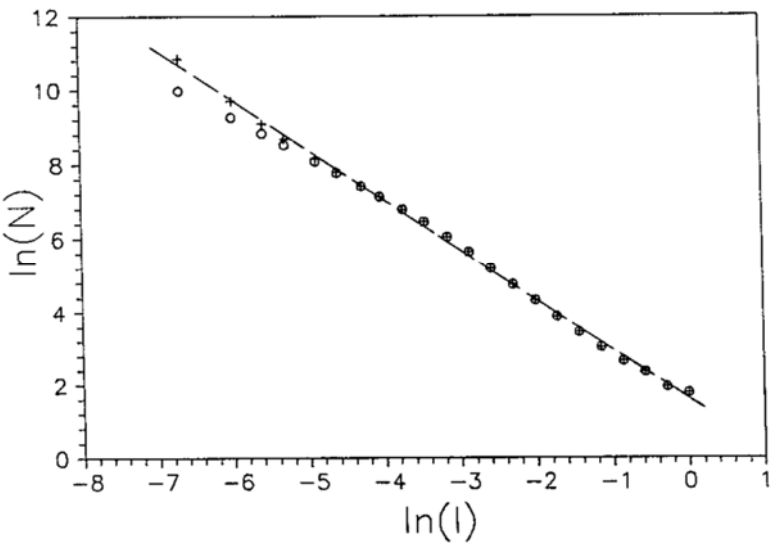

„fractal dimension“ = 1.4

modeling by introducing on the crack surface a damage variable that accumulates stress-induced corosion

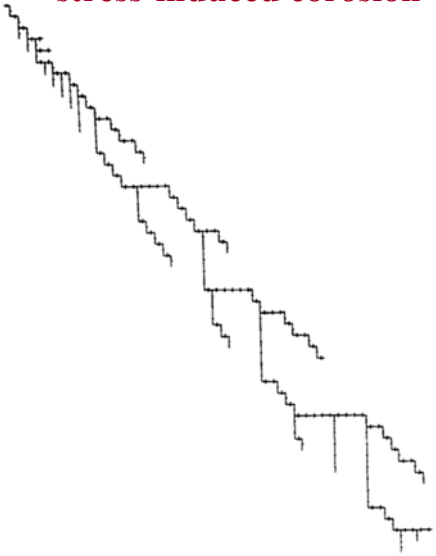

Fragmentation

Volcanic Fragments

Fragment Size Distributions

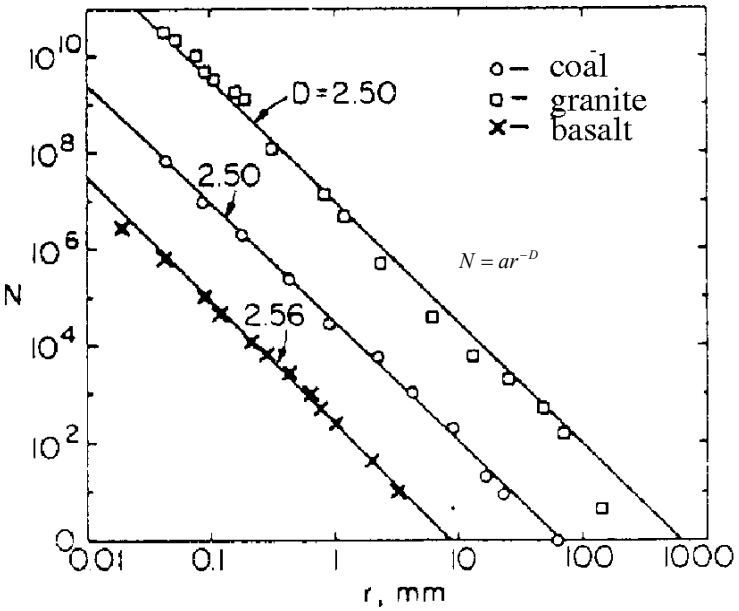

$$N = ar^{-D}$$

Turcotte (86)

Impact of plaster discs

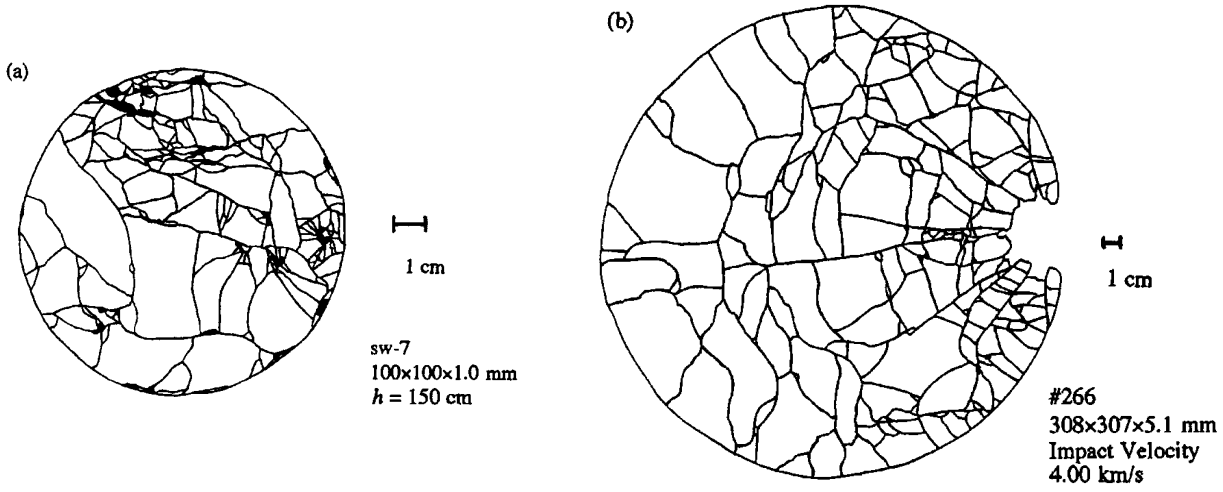

Kadono (97)

Fragment Size Distributions

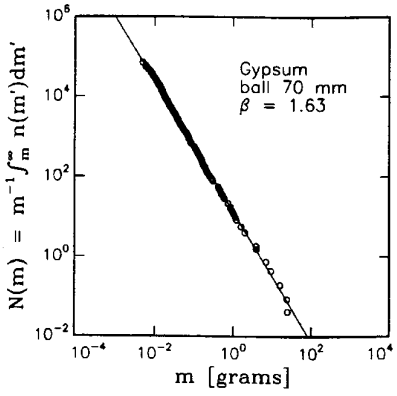

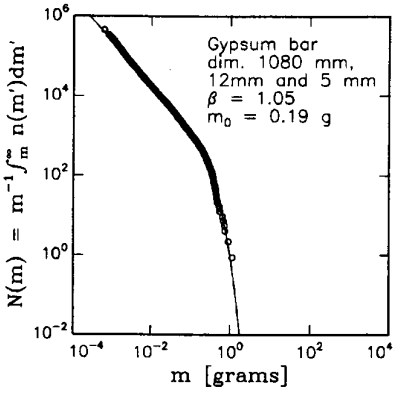

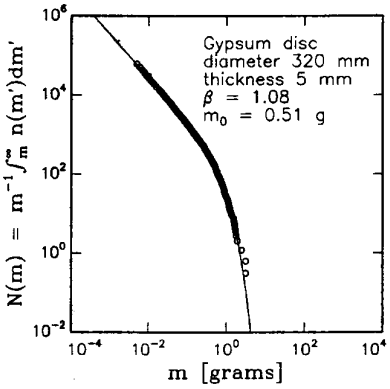

Oddeshede (93)

Discrete Elements

Alder and Wainwright (1957)

= deterministic simulation of the motion of a classical many body system

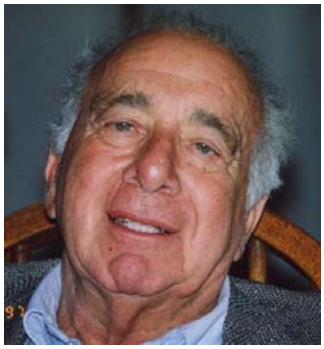

Bernie Alder

- **Newtonian mechanics**
- **Conservation of energy and momentum**
- **Invariance under translation and rotation**

M.P. Allen and D.J. Tildesley: „Computer Simulation of Liquids“ (Clarendon Press, Oxford, 1987)

Equations of motion

Solve Newton's equation:

$$\dot{\vec{x}}_i = \vec{v}_i = \frac{\vec{p}_i}{m_i} \quad , \quad \dot{\vec{p}}_i = -\vec{\nabla}_i V(Q) = \vec{f}_i$$

$$m_i \ddot{\vec{x}}_i = \vec{f}_i = \sum_j \vec{f}_{ij} \qquad i = 1, \ldots, N$$

vector sum of all forces that act on particle *i*.

system of *N* coupled equations

Solving the equations

- **Euler method**
- **Runge Kutta method**
- **Predictor-Corrector method**
- **Verlet method**
- **Leap-frog method**

special for Newton eqs.

Verlet method

ETH

Loup Verlet (1967)

real time

$\Delta t \approx t_c/20$

Taylor expansion in time step Δt:

$$\vec{x}(t+\Delta t) = \vec{x}(t) + \Delta t\ \vec{v}(t) + \frac{1}{2}\Delta t^2\ \dot{\vec{v}}(t) + \ldots$$

$$\vec{x}(t-\Delta t) = \vec{x}(t) - \Delta t\ \vec{v}(t) + \frac{1}{2}\Delta t^2\ \dot{\vec{v}}(t) + \ldots$$

add the two equations $\Rightarrow$

from Newton equation

$$\vec{x}(t+\Delta t) = 2\vec{x}(t) - \vec{x}(t-\Delta t) + \Delta t^2 \ddot{\vec{x}}(t)$$

Rotations in two dimensions

ETH

Time evolution of the rotation angle φ using the Verlet algorithm:

$$\varphi(t+\Delta t) = 2\varphi(t) - \varphi(t-\Delta t) + \Delta t^2 \frac{T(t)}{I}$$

with

$$T(t) = \sum_{j \in A} \left(f_j^y(t) \cdot d_j^x(t) - f_j^x(t) \cdot d_j^y(t) \right)$$

ω = angular acceleration

x-component of the vector connecting the center of mass to the mass element j

DEM of Polygons

$$\vec{F}_i = \sum_j \vec{F}_{ij} + m_i \vec{g} \qquad T_i = \sum_j T_{ij}$$

$$\vec{x}_i(t+1) = \vec{x}_i(t) + \vec{v}_i(t)\Delta t$$

$$\vec{v}_i(t+1) = \vec{v}_i(t) + \frac{\vec{F}_i}{m_i}\Delta t$$

$$\varphi_i(t+1) = \varphi_i(t) + \omega_i(t)\Delta t$$

$$\omega_i(t+1) = \omega_i(t) + \frac{T_i}{I_i}\Delta t$$

two dimensions

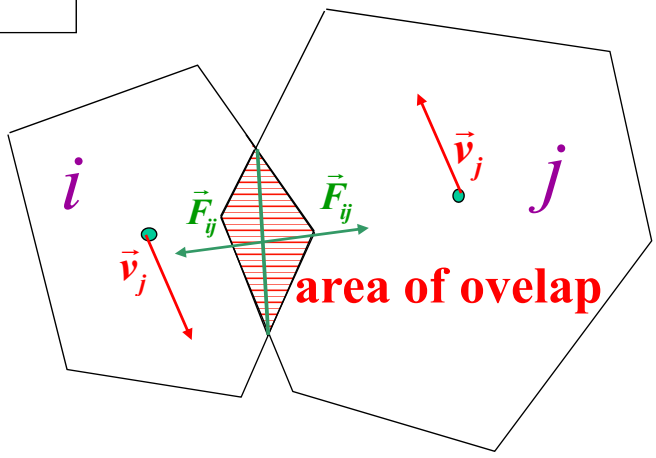

Cundall and Strack:

$$\overrightarrow{F_{ij}} = -\frac{YA}{l}\vec{n} - \gamma v_{ij}^{(n)}\vec{n} - \min\left(\gamma v_{ij}^{(t)}, \mu F_{ij}^{(n)}\right)\vec{t}$$

Inelastic collisions

The restitution coefficient *r* can be measured by letting the particle fall from a height $h^{initial}$ on a plate of same material and measuring the rebounce height h^{final}:

$$r = r_n = \frac{E^{after}}{E^{before}} = \frac{h^{final}}{h^{initial}} = \left(\frac{v_n^{after}}{v_n^{before}}\right)^2$$

One also defines normal and tangential coefficients:

$$e_n = \sqrt{r_n} = \frac{v_n^{after}}{v_n^{before}} \quad , \quad e_s = \sqrt{r_s} = \frac{v_s^{after}}{v_s^{before}}$$

Restitution Coefficient

	e_n
steel	0.93
aluminum	0.8
plastic	0.6

Simulation of Impacting Disc

Potapov et al (95)

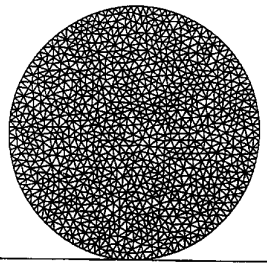

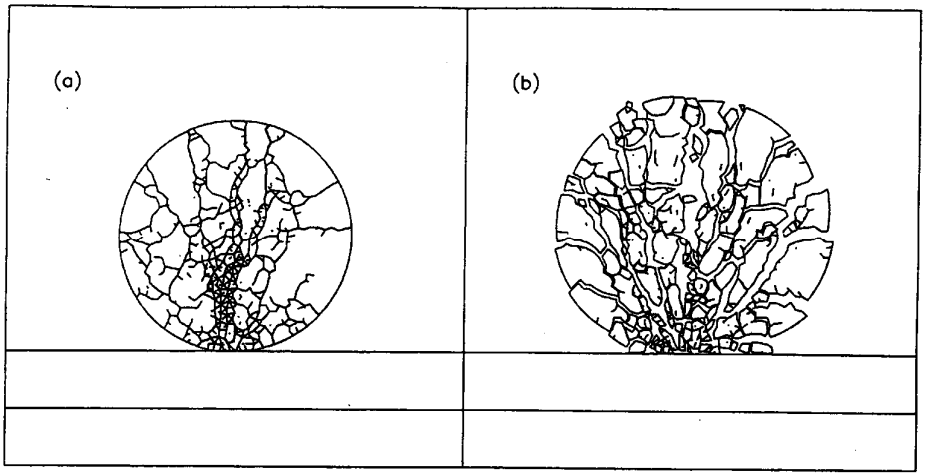

Two colliding discs

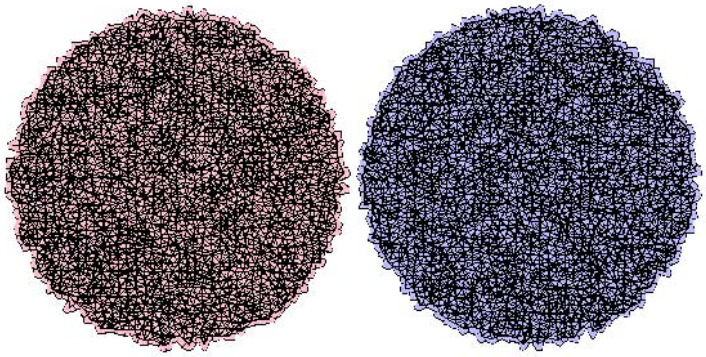

Three Snapshots

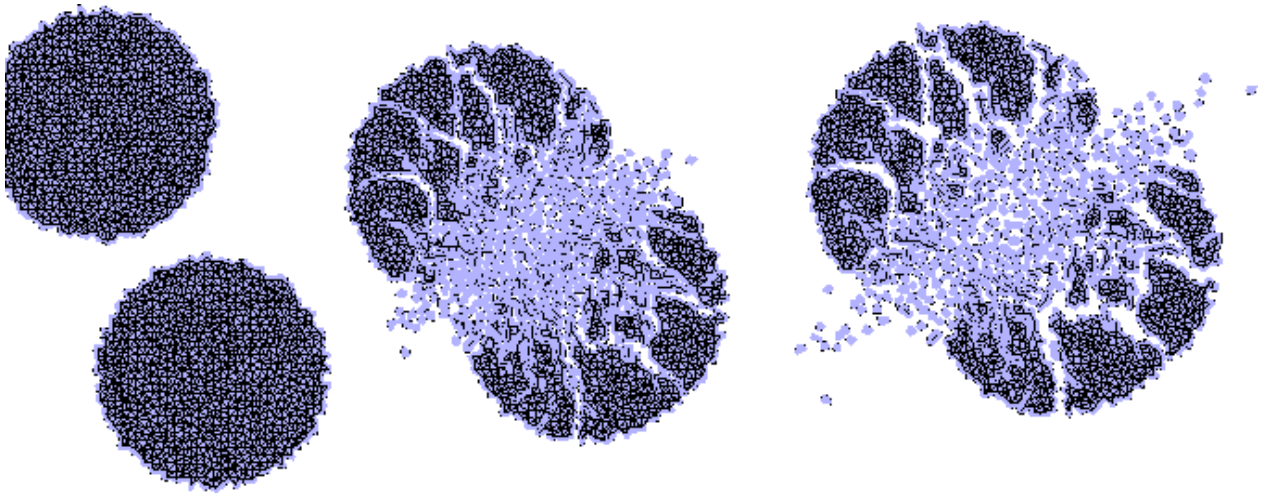

Velocities for three different impact parameters

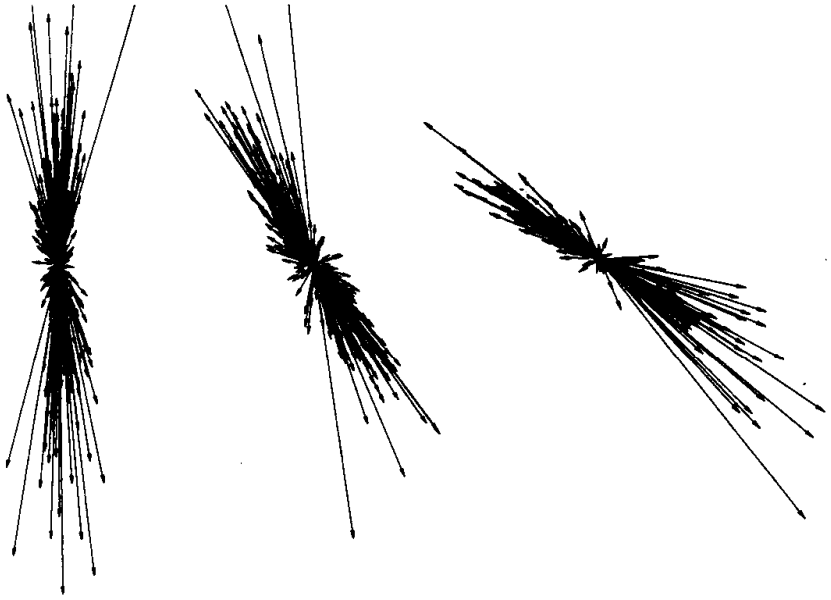

b/d=0 b/d=1/3 b/d=2/3

Distributions of Fragment Velocities

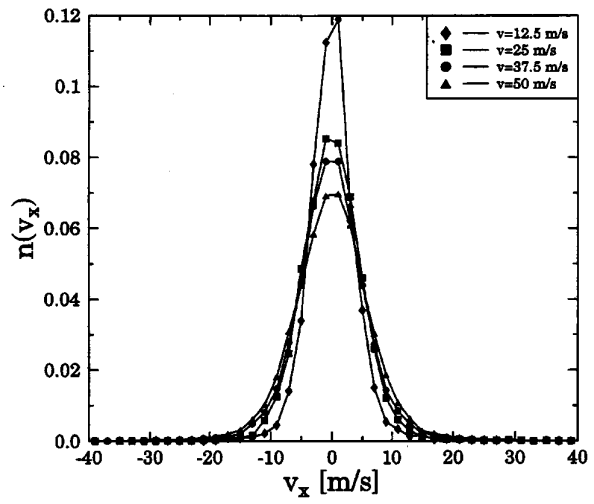

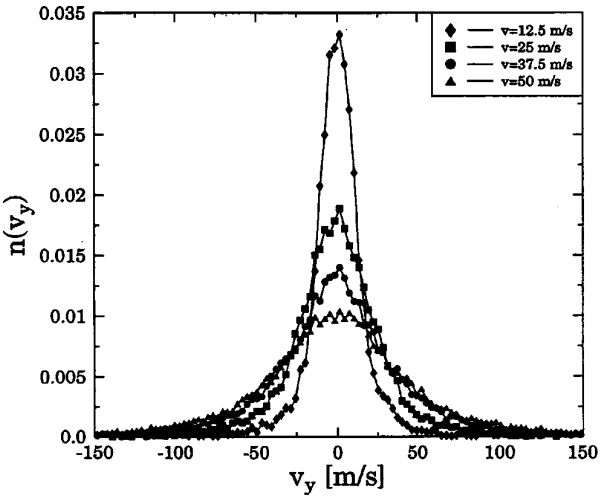

Scaling of Velocity Distributions

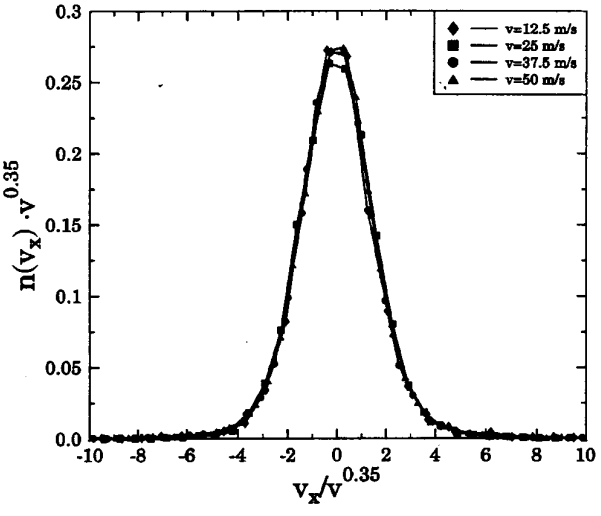

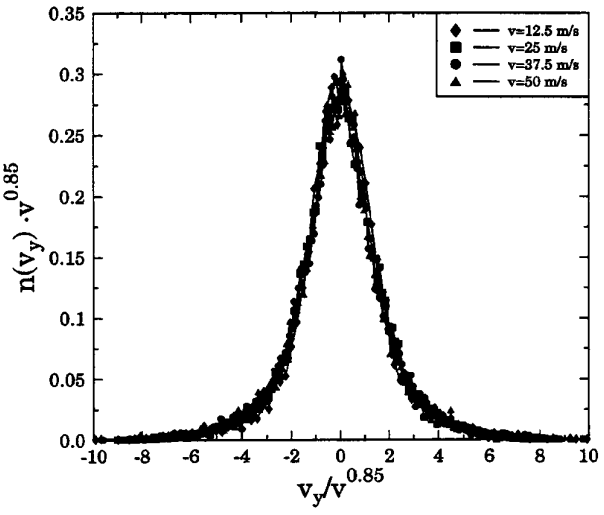

Fragment Mass Distributions

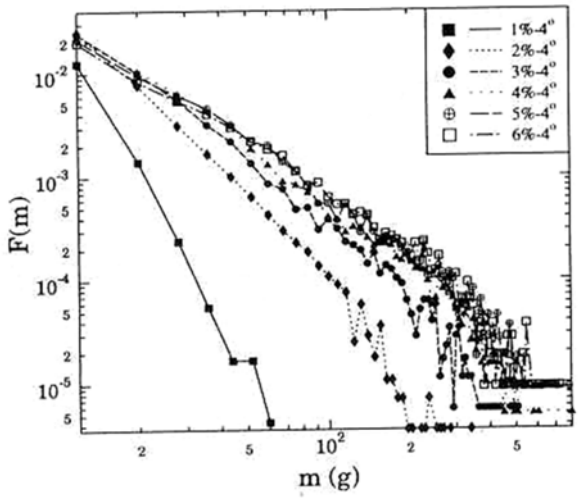

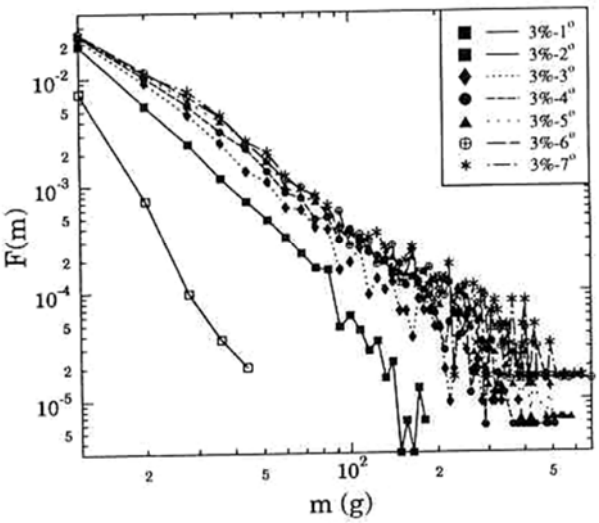

Mass of largest fragment

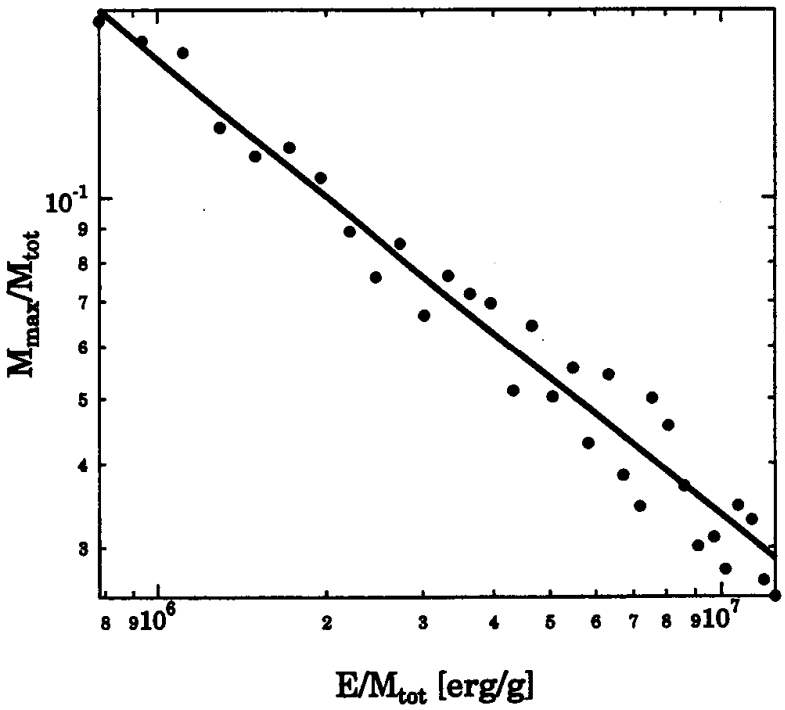

Dependence on Disk Size

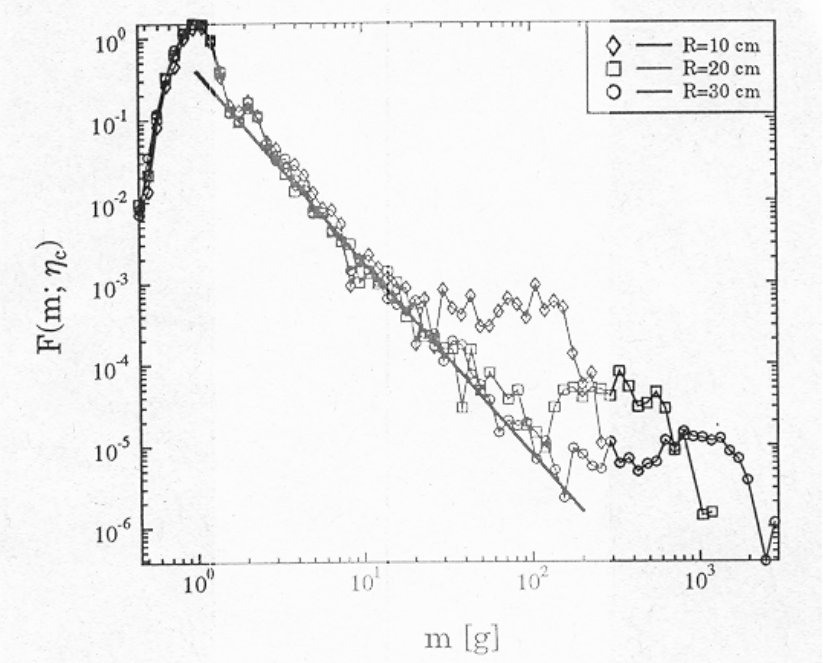

FIG. 8. Mass distribution of fragments at the transition point η_c for three different values of the system size R.

Released Energy

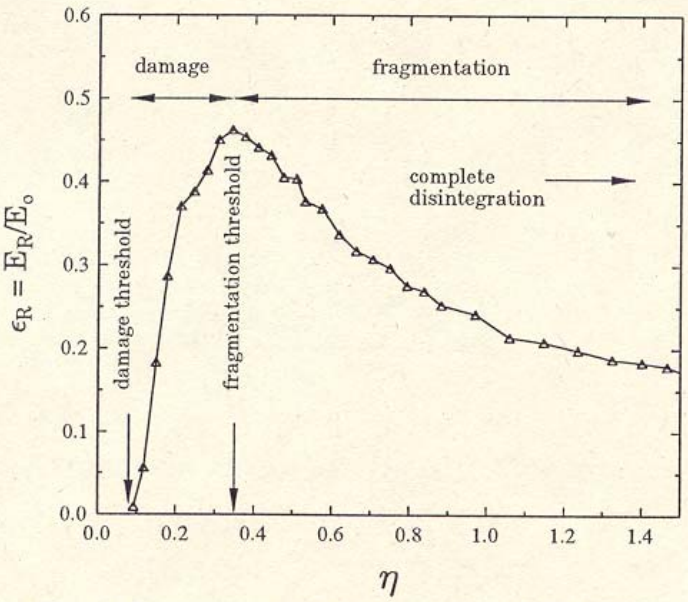

FIG. 4. The ratio ϵ_R of the energy released by breaking E_R and the total kinetic energy E_o. The transition point (fragmentation threshold) between the damaged and fragmented states is identified with the position of the maximum of ϵ_R.

Proportion of the Largest Masses

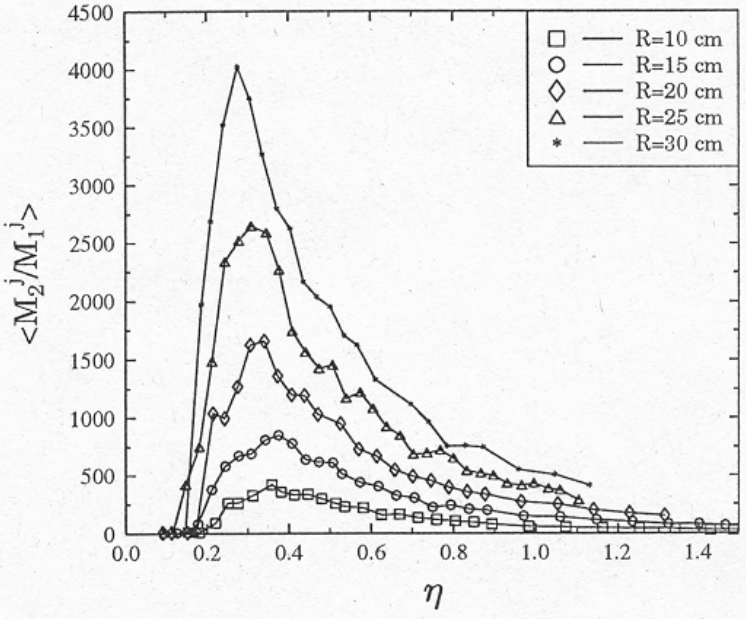

FIG. 9. $\left\langle M_2^j/M_1^j \right\rangle$ as a function of η for five different values of R.

Simulation of Ball Mill

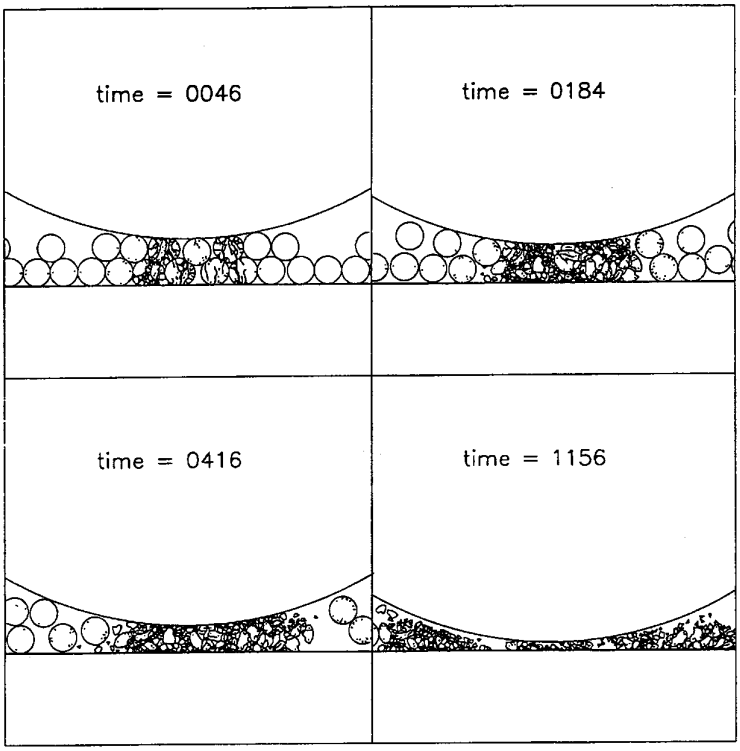

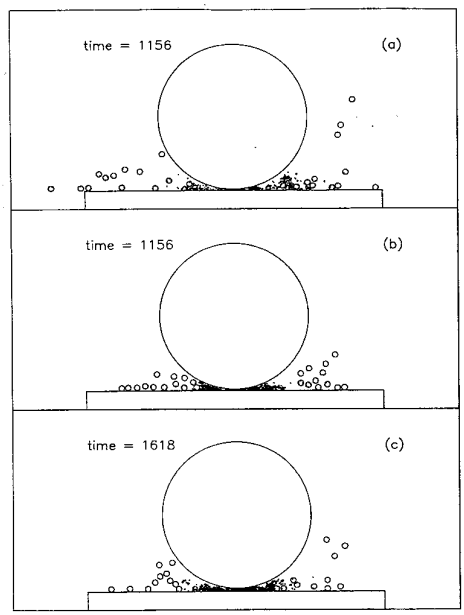

Potapov et al (95)

Simulation of Ball Mill

Role of agglomeration

Low Cohesion

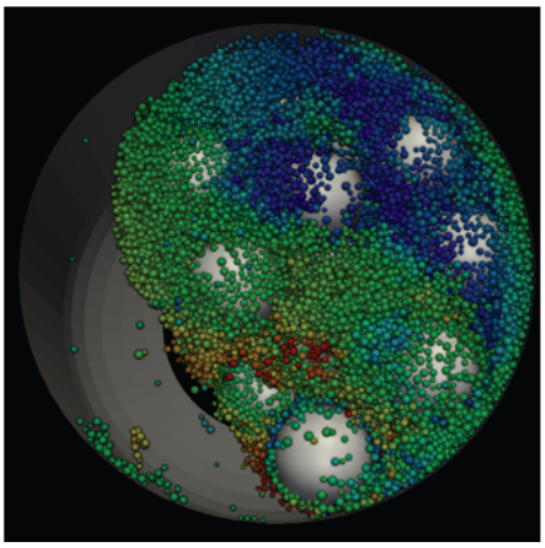

High Cohesion

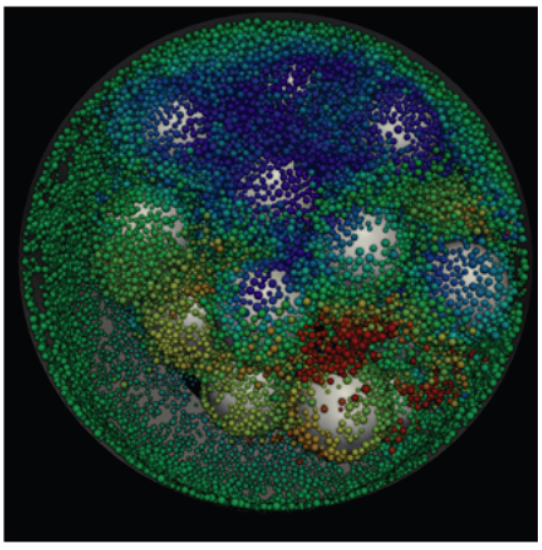

Simulation of Ball Mill

System Construction: Insilico Clinker

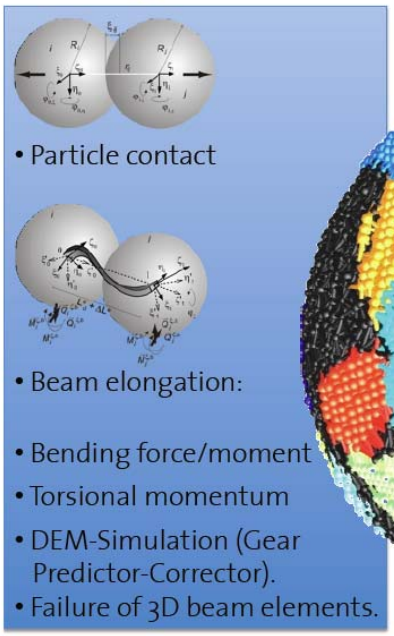

- Particle contact

- Beam elongation:
- Bending force/moment
- Torsional momentum
- DEM-Simulation (Gear Predictor-Corrector).
- Failure of 3D beam elements.

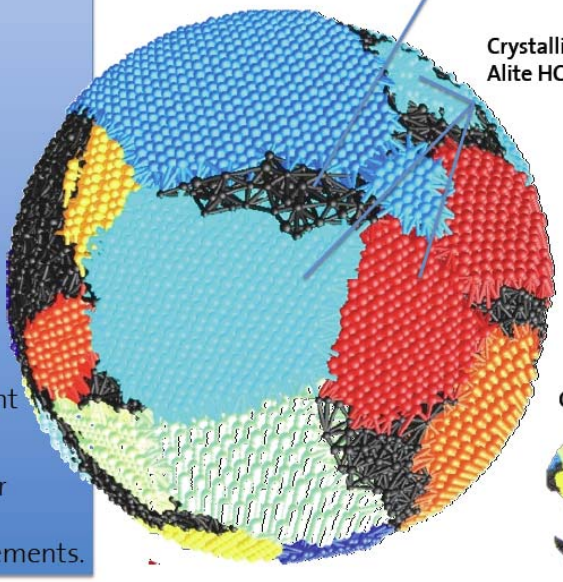

Cross section:

Hitting a Wall

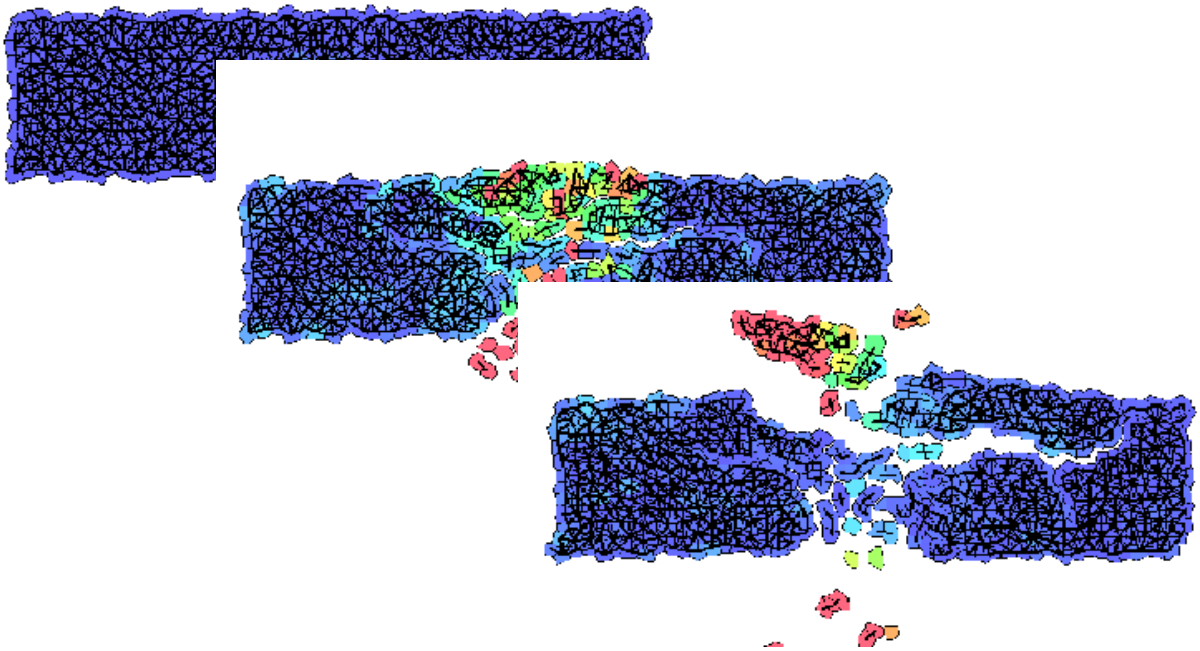

Explosion of a Disk

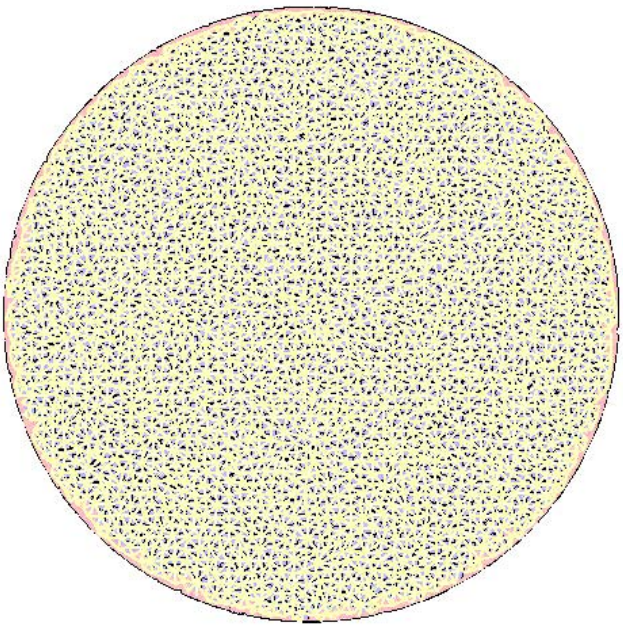

Pendulum Impact

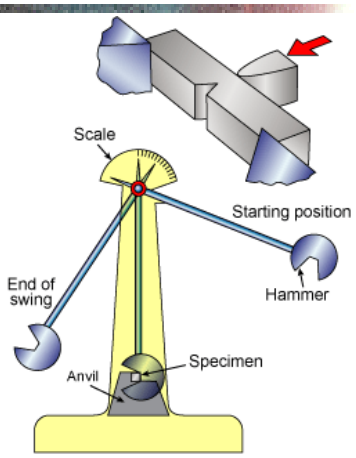

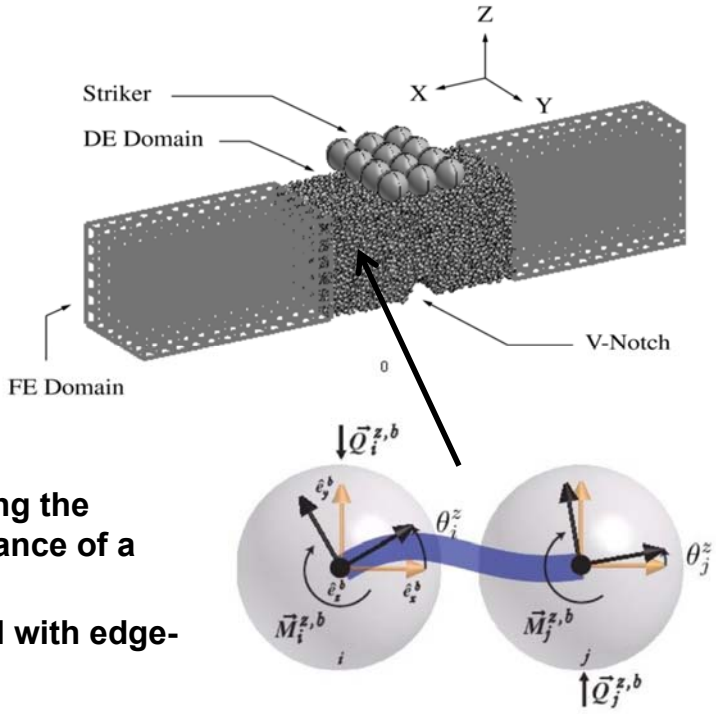

- Classic test for determining the dynamic impact resistance of a material
- Hybride DEM / FEM model with edge-to-edge coupling

Pendulum Impact

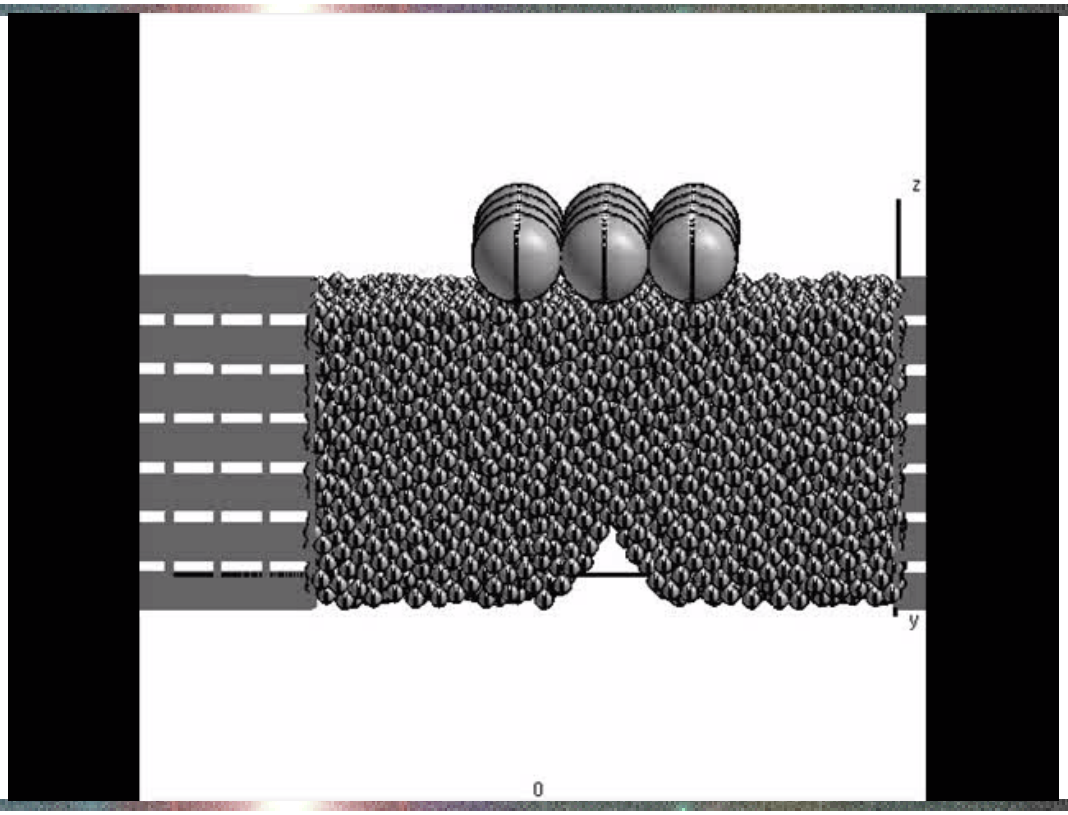

Fragmentation of Shells

space debris

Height Distribution of Space Debris

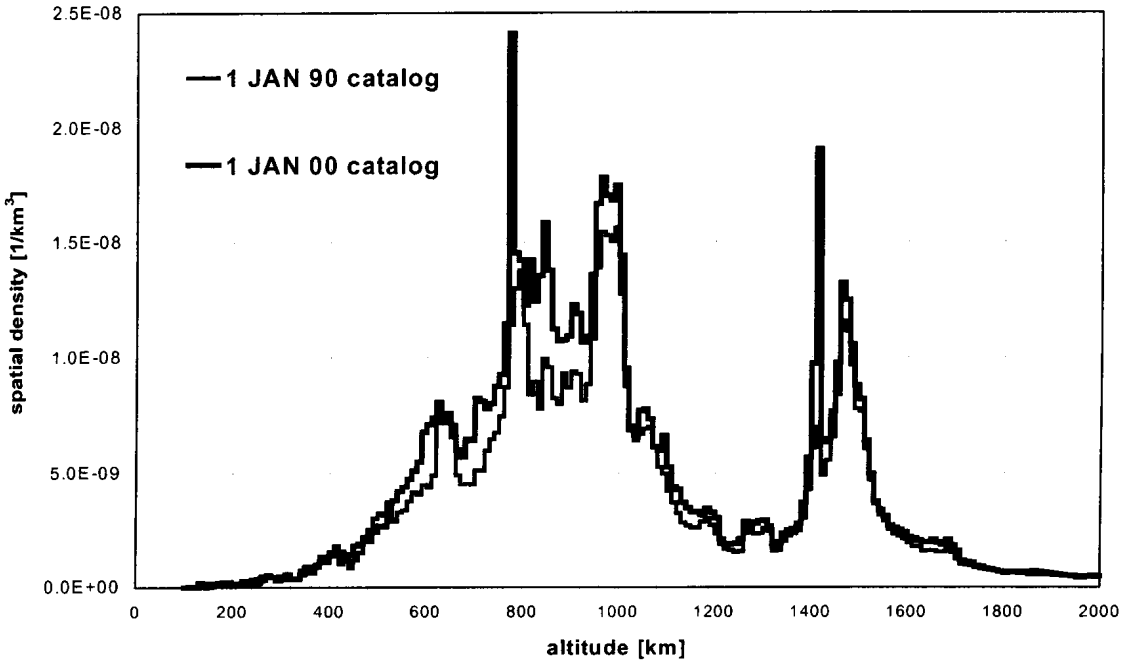

Fig. 1. The LEO spatial density in 1990 and 2000

Area and Mass Distribution

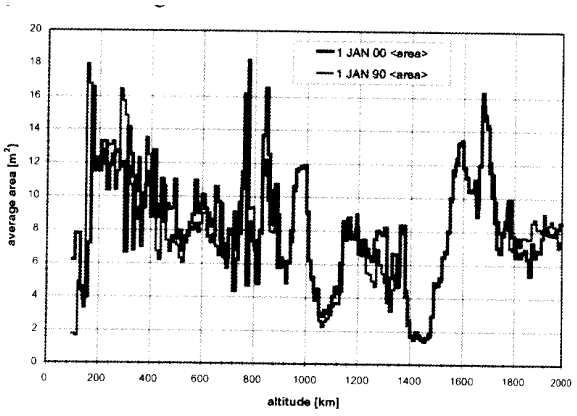

Fig. 2. Area distribution in LEO

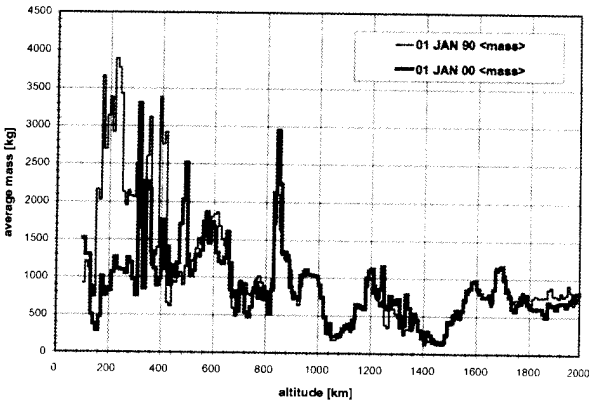

Fig. 3. Mass distribution in LEO

Breaking Glass Pipes

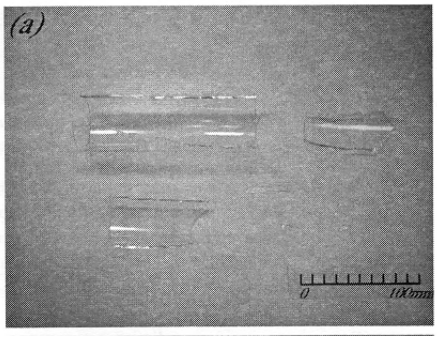

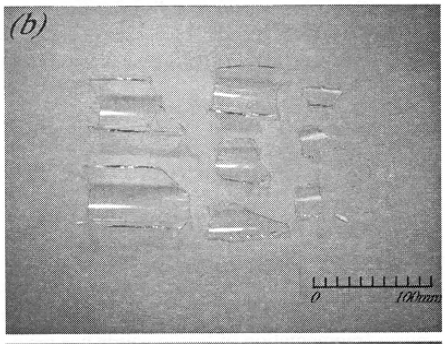

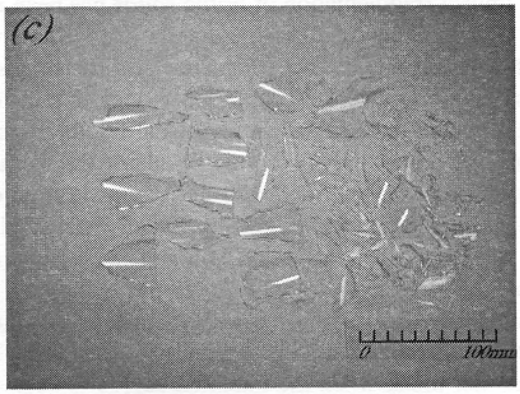

Kasuragi et al (03)

Experiments on Shell Fragmentation

- **materials (crystaline,amorphus,brittle,disordered)**
- **length scale**
- **way of imparting energy (impact,explosion)**

Experiments for Shell Fragmentation

impact

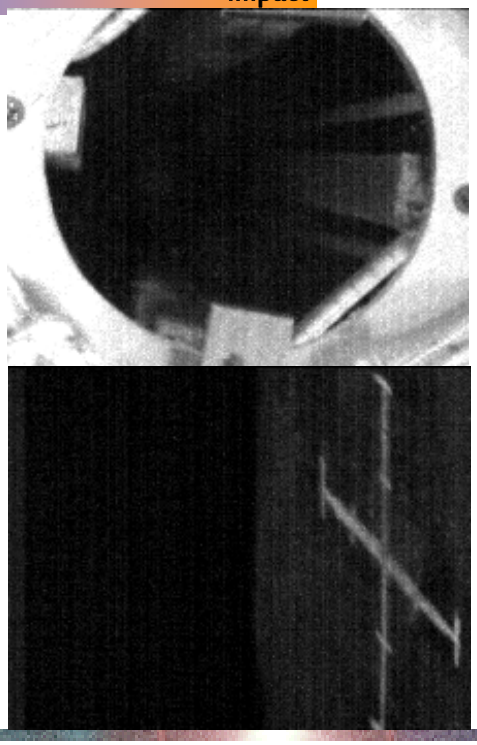

explosion

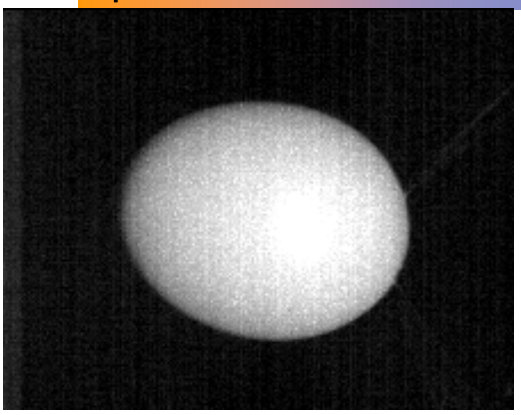

Cardboard Box

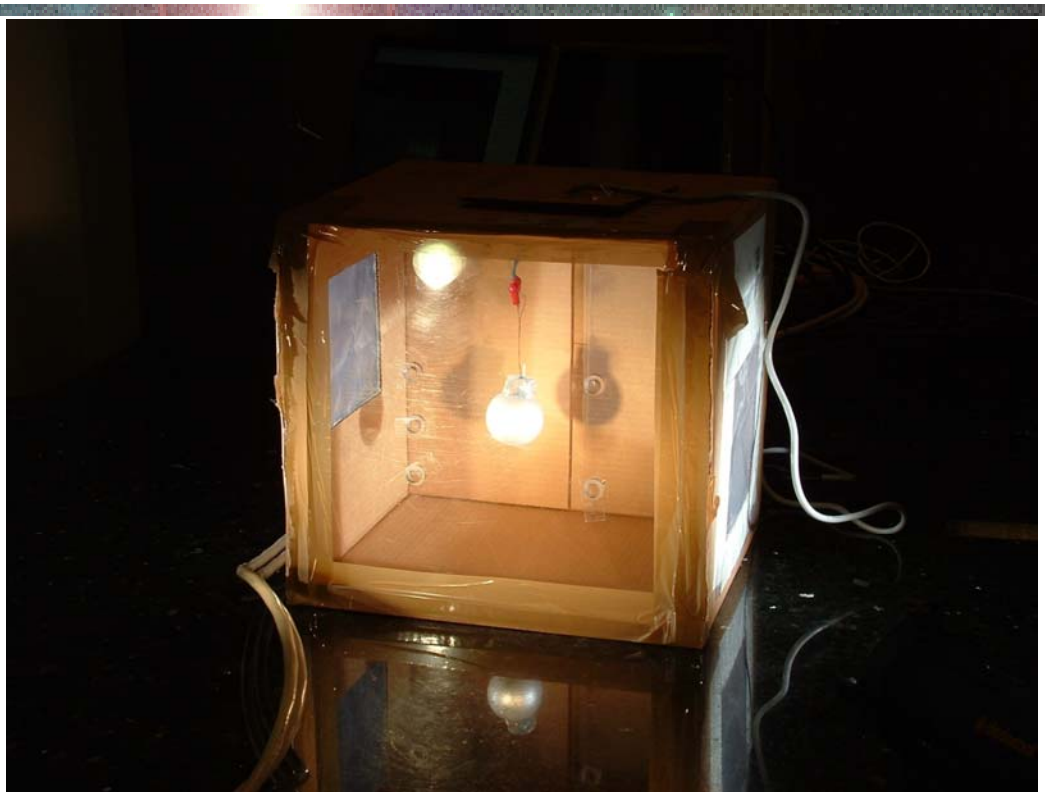

Explosion of an Egg

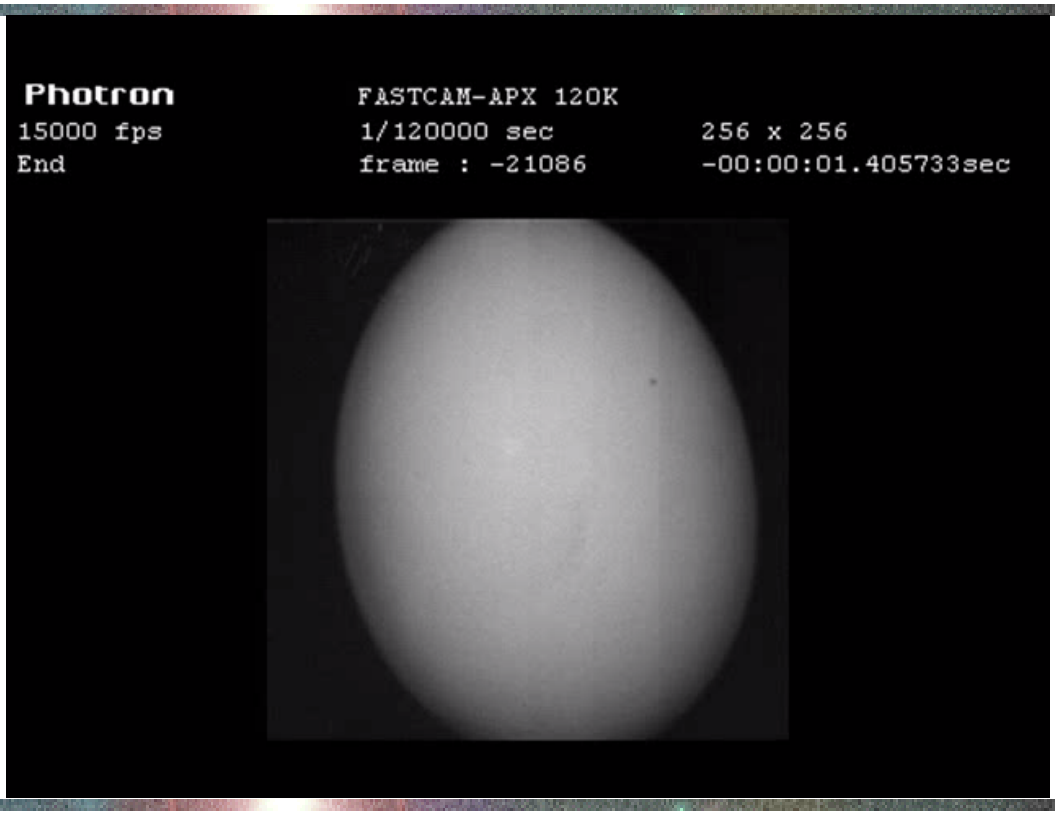

Explosion of a Christmas Glitter Ball

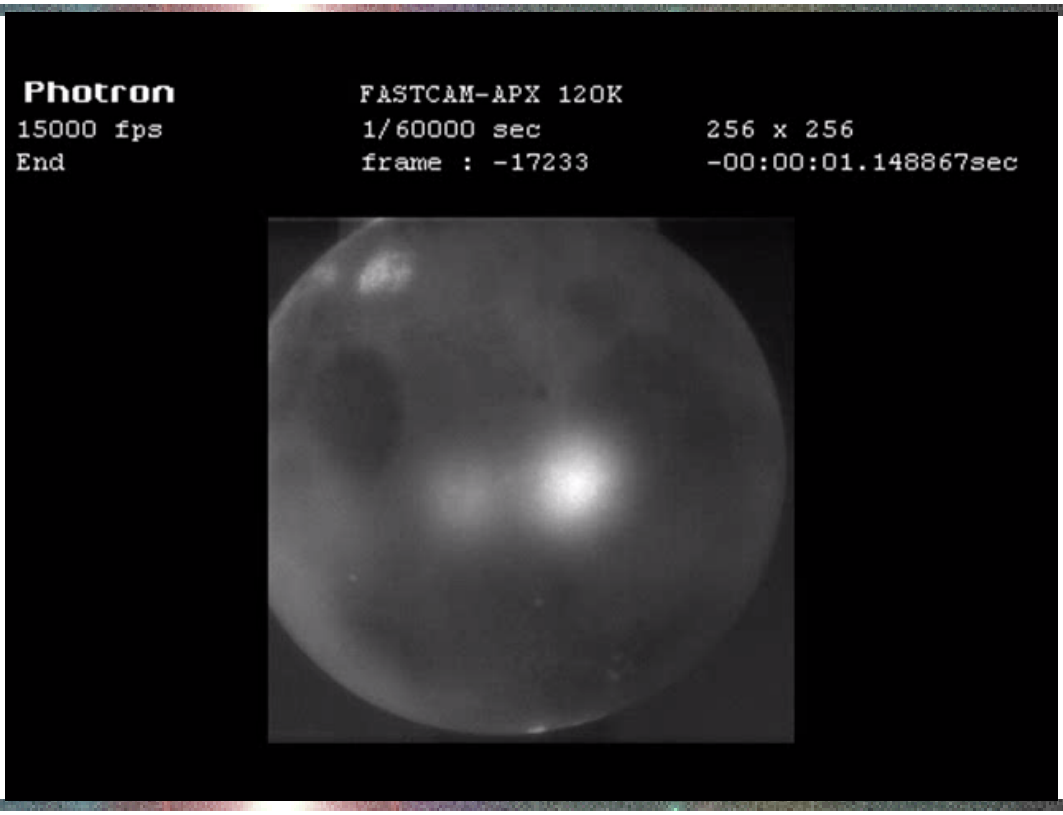

Exploding Balloon

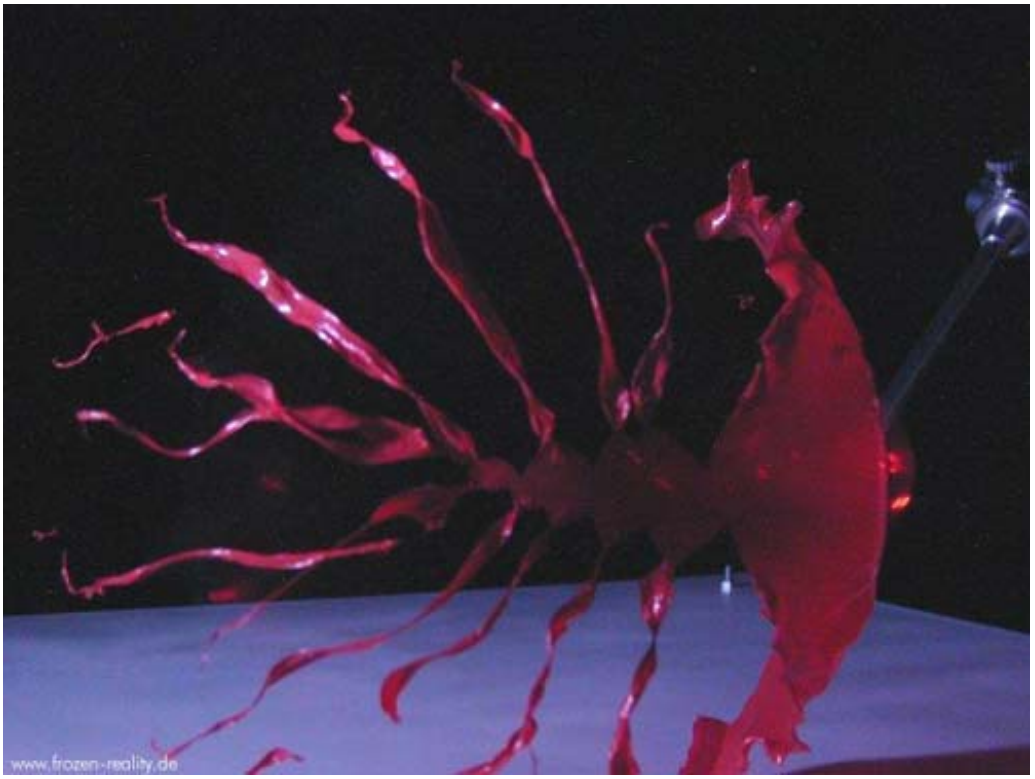

Analyzing the Fragments

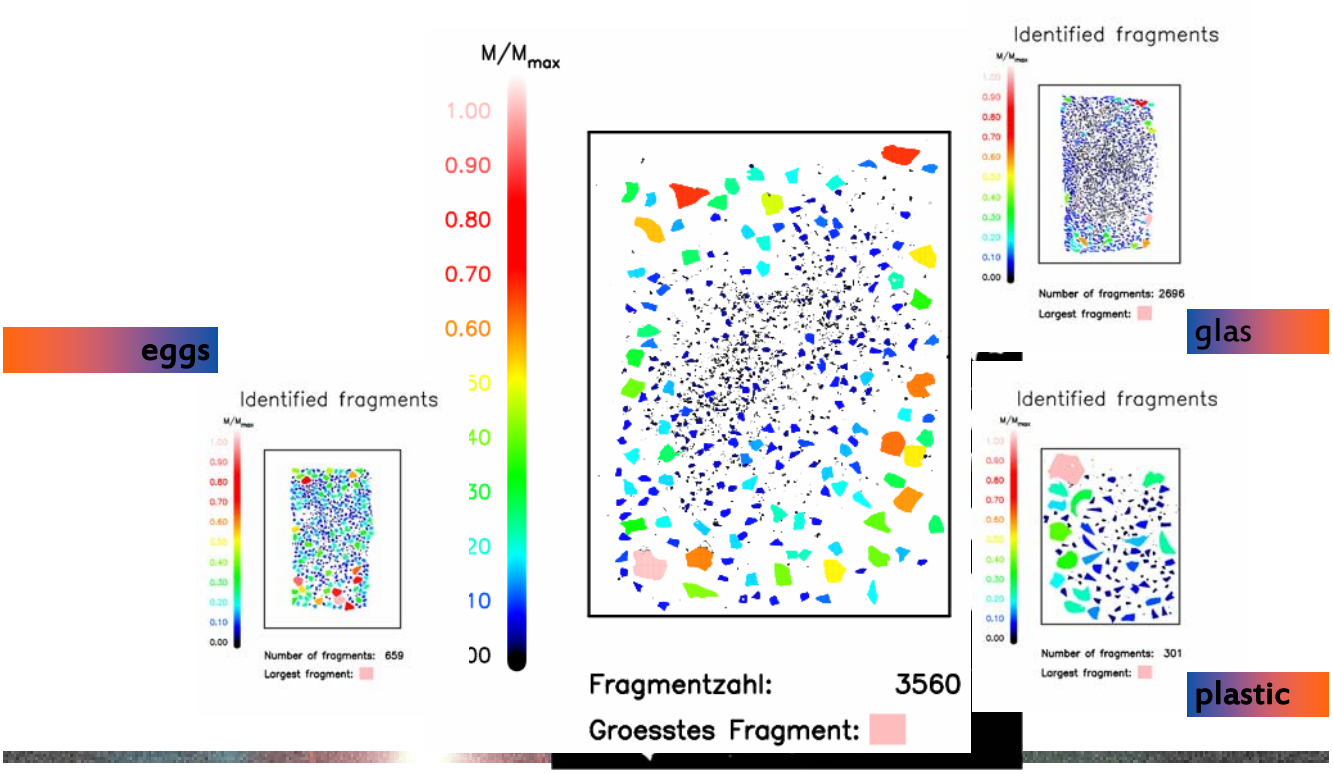

Fragment Mass Distributions

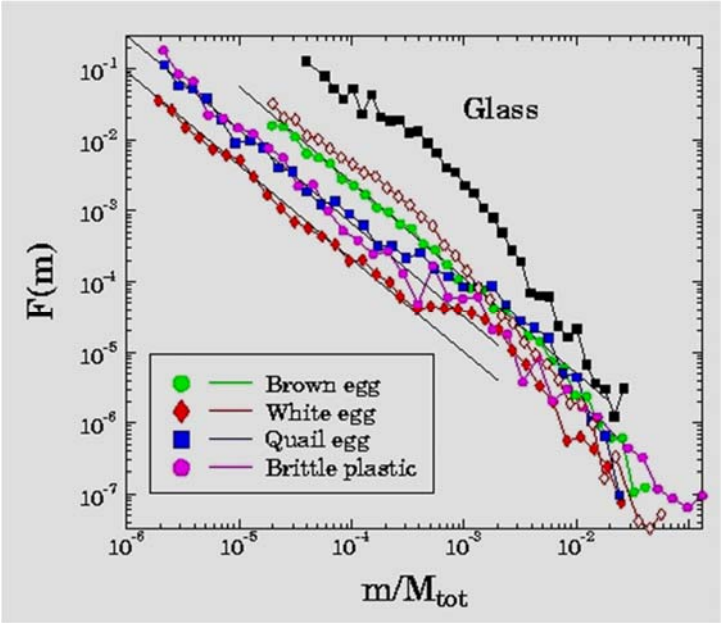

Shape of Fragments

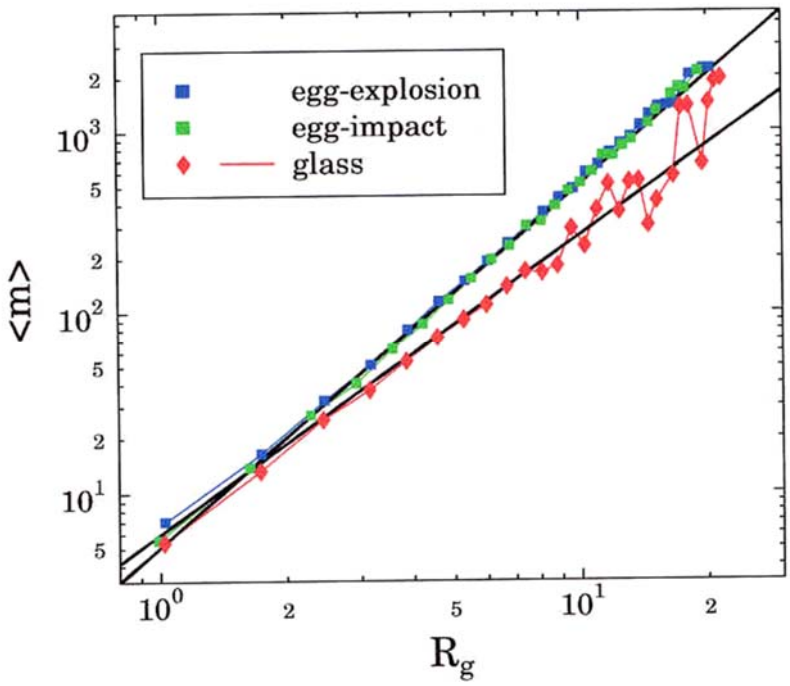

Distribution of area/mass

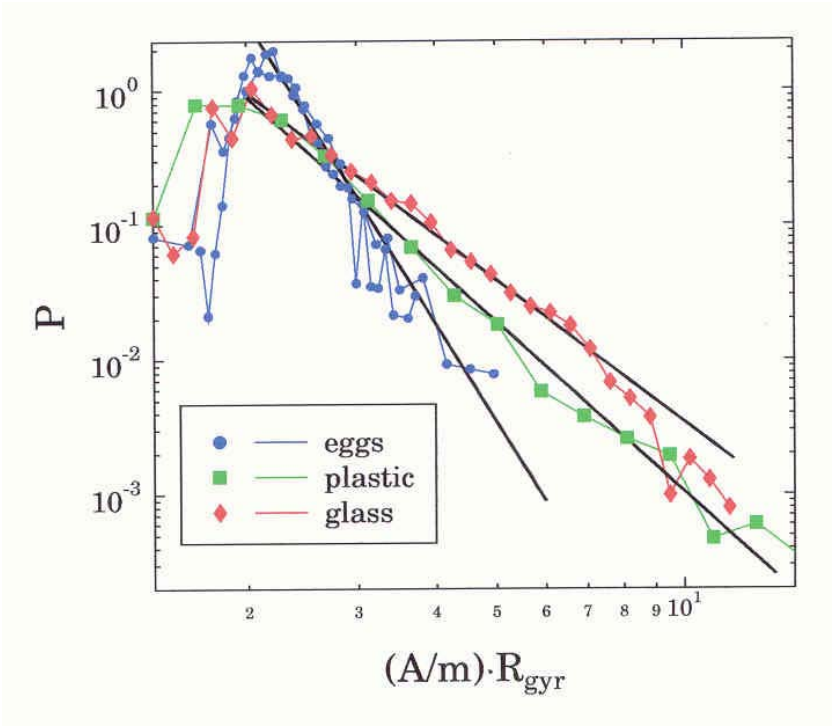

Shell Model

- triangulated sphere
- pressure acts on triangle
- adiabatic system

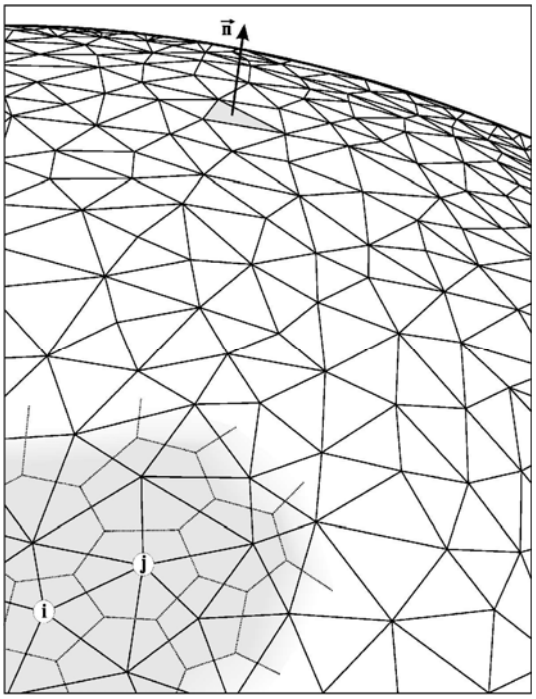

Simulation of Fragmentation

ETH

280 Pa

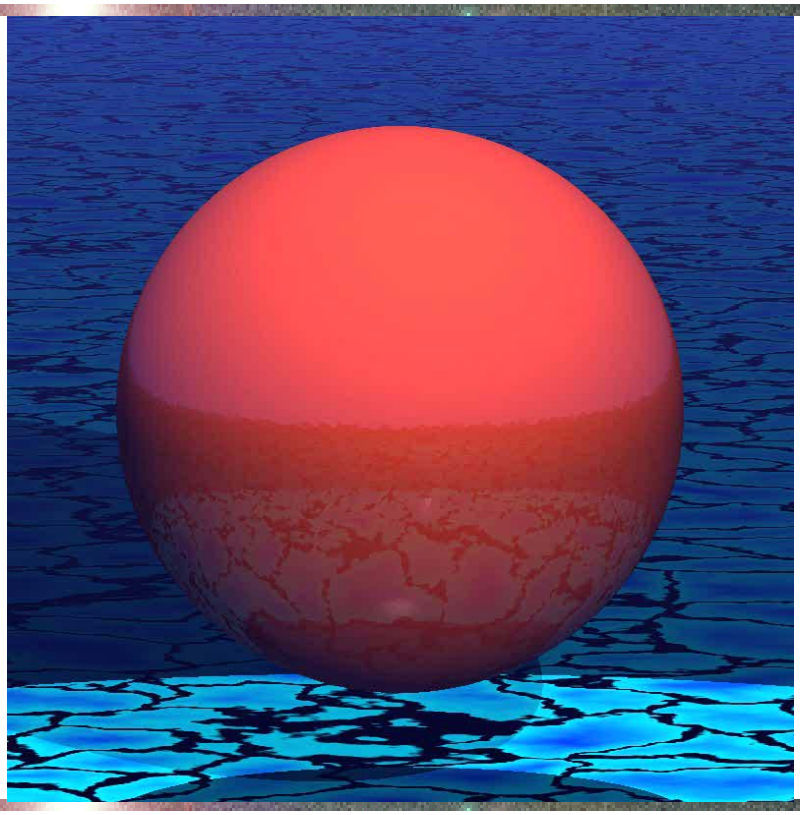

Simulation of Fragmentation

ETH

400 Pa

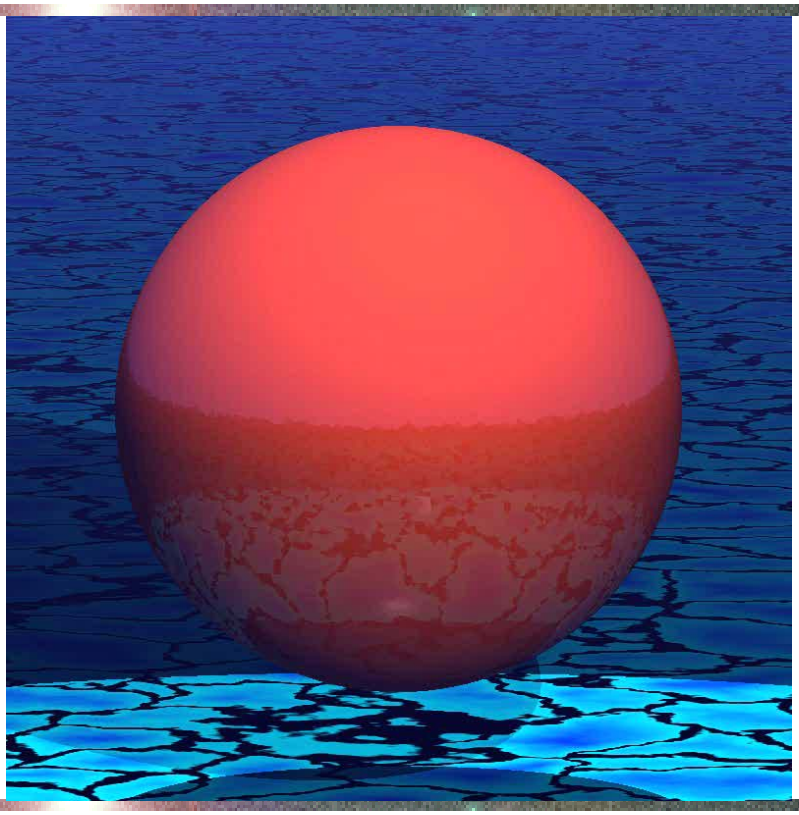

Simulations Varying Wall Thickness

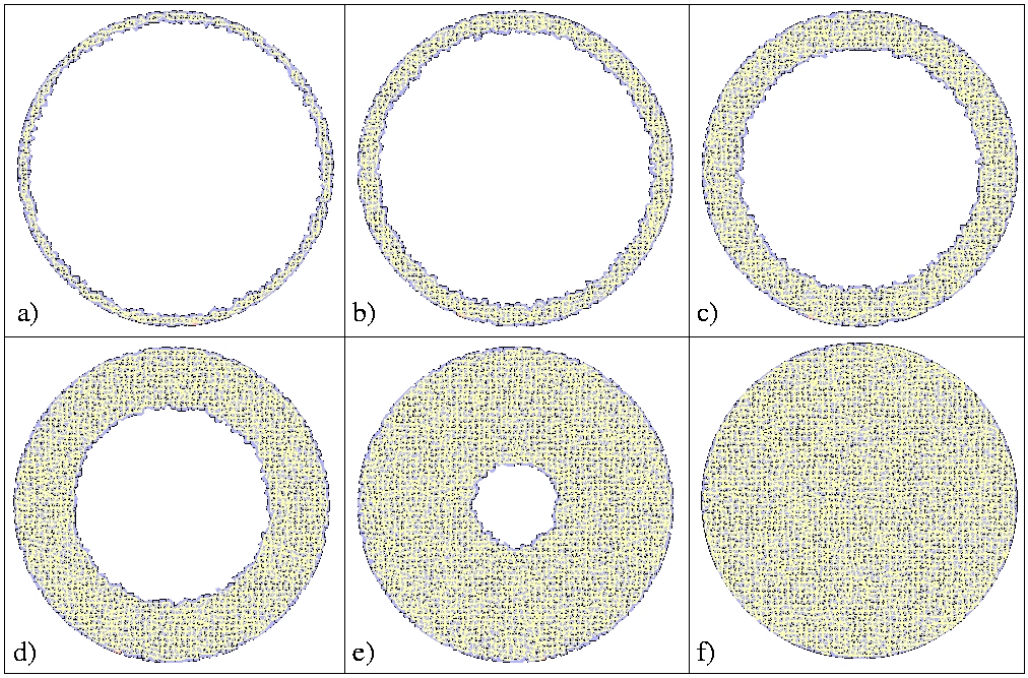

Thin Shell

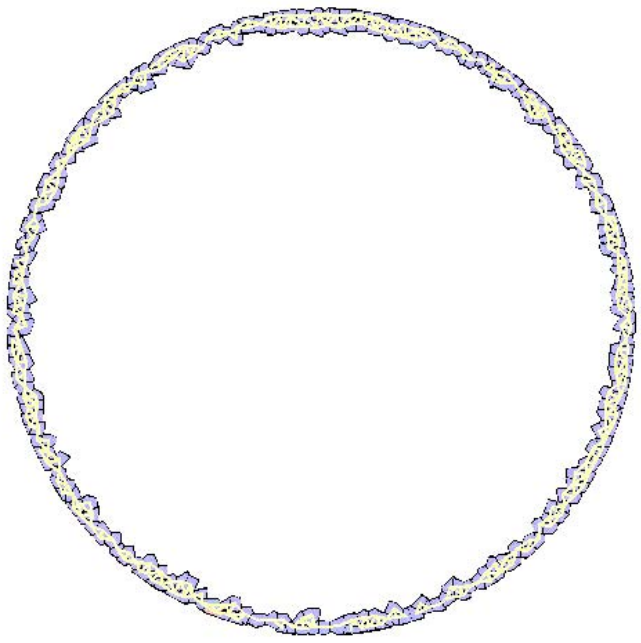

Thick Shell

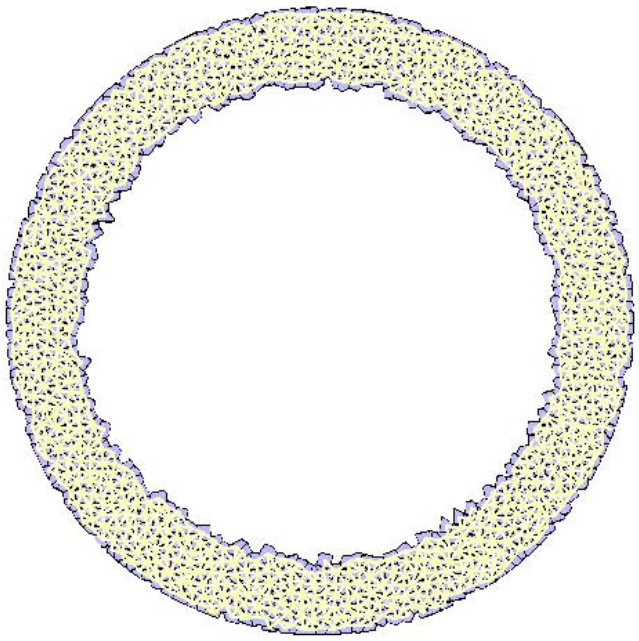

Very Thick Shell

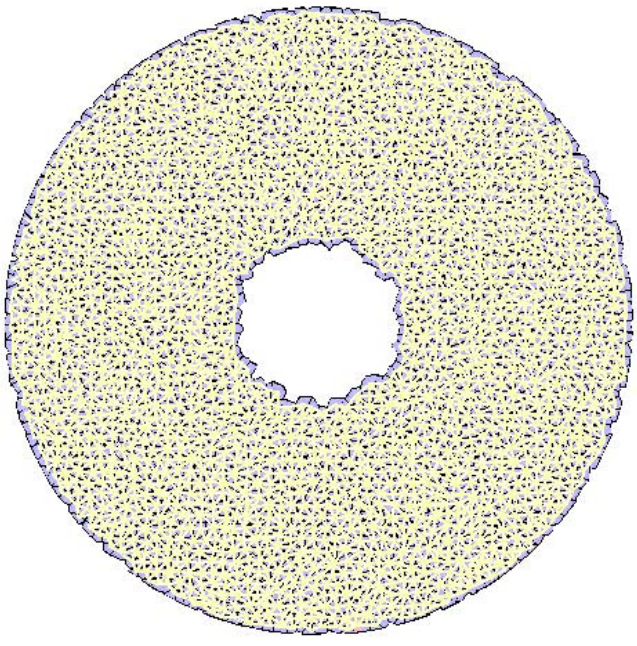

Fragmentation in shear bands

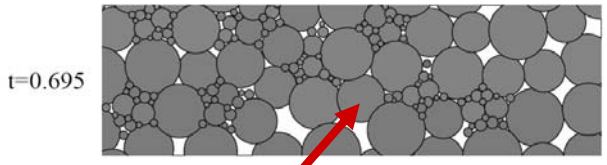

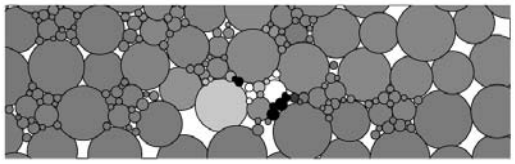

fragments

Shear bands become denser and stiffer

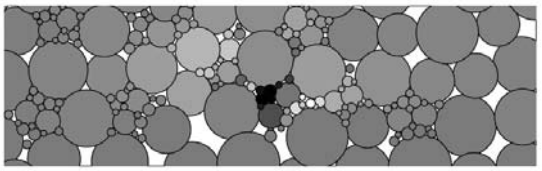

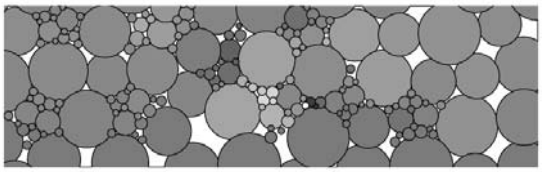

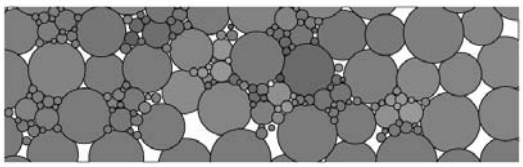

Jan Astrom